UNIVERSITY OF CALIFORNIA

Santa Barbara

Microcrystals promote cystogenesis and exacerbate autosomal dominant polycystic kidney disease

A dissertation submitted in partial satisfaction of the requirements for the degree Doctor of Philosophy in Molecular Cellular and Developmental Biology

by

Jacob Alexander Torres

Committee in charge:

Professor Thomas Weimbs, Chair

Professor Kathy Foltz

Professor Dzwokai (Zach) Ma

Professor Joel Rothman

March 2017

The dissertation of Jacob Torres is approved by

_____

Professor Thomas Weimbs

_____

Professor Kathy Foltz

_____

Professor Dzwokai (Zach) Ma

_____

Professor Joel Rothman

March 2017

Microcrystals promote cystogenesis and exacerbate autosomal dominant polycystic kidney disease

ACKNOWLEDGEMENTS

I would like to acknowledge the support of my family, friends, and loved ones, those that I have had the fortune to meet along this long and at times difficult journey, those that I have lost along the way, those that have always been there to listen, provide guidance, advice and support. Without all of them I could not have succeeded.

-Thank you all

VITA OF Jacob Alexander Torres
March 2017

EDUCATION

Bachelor of Arts in Biology, University of California, Riverside, March 2010
Master of Arts in Molecular Cellular and Developmental Biology, University of California, Santa Barbara, June 2014
Doctor of Philosophy in Molecular Cellular and Developmental Biology, University of California, Santa Barbara, June 2017

PROFESSIONAL EMPLOYMENT

2010-2016: Teaching Assistant, Department of Molecular Cellular and Developmental Biology, University of California, Santa Barbara
Courses: General Biology Lab, General Biochemistry, Oncogenesis, Physiology, Genetics, Neurodevelopment, Immunology, Contemporary Nutrition, Cellular Biology, Cellular Biology Lab

2011-2013: Mentor, Summer Mentorship Program; Summer Sessions, University of California, Santa Barbara

PUBLICATIONS

AWARDS

Mentor Summer Research Internship Program, University of California, Riverside 2009

Bridge to Doctorates Fellowship, University of California, Santa Barbara, 2010

Graduate Opportunity Fellowship, University of California, Santa Barbara, 2012 & 2013

Doreen Putrah Travel Fellowship, University of California, Santa Barbara, 2015 & 2016

FIELDS OF STUDY

Major Field: Cellular Biology

ABSTRACT

Microcrystals promote cystogenesis and exacerbate autosomal dominant polycystic kidney disease

by

Jacob Alexander Torres

Autosomal Dominant Polycystic Kidney Disease (ADPKD) is a genetic disorder affecting approximately 2.5 million people worldwide. It is the number one, life-threatening monogenic disorder known, caused by mutations in either the *Pkd1* or *Pkd2* genes resulting in numerous fluid-filled cysts within the kidneys. ADPKD presents in the 2nd decade of life and presents with progressive renal decline and eventually to end stage renal disease (ESRD) in the 5th to 6th decade of life for half of all patients. Currently no treatments exist to ameliorate or cure ADPKD, creating a large financial burden on both the health care system, the patient, and their care-givers[1]. Treatment options once patients reach ESRD are limited to dialysis and kidney transplant. Since the discovery of the genetic link to ADPKD, there has been intense research to understand what role the *Pkd1/2* genes play in the formation of cysts and the progression of ADPKD. The slow progression of ADPKD and the difference in disease severity between individuals implies that there may be environmental factors acting as causative agents in promoting cyst formation[2]. Animal models of ADPKD appear to be more susceptible to cyst formation following injury with nephrotoxic chemicals, ischemia, and partial or total unilateral nephrectomy[3–5]. These data demonstrate that the injured state is

a driver of cyst formation once *Pkd1/2* have been mutated, but these experimental approaches are not representative of normal environmental injuries to the kidney. The focus of my research is to elucidate an environmental agent that can promote cystogenesis in an otherwise healthy individual. The kidney is responsible for filtering solutes from the blood which include ions and molecules that under the right circumstances can form precipitates in the urinary filtrate. It is our hypothesis that the endogenous kidney injury in ADPKD patients results via the precipitation of microcrystals and the inappropriate response to crystal clearance. The kidney is producing sub-clinical microcrystals daily that are excreted into the urine without incident. Individuals with ADPKD may be unable to respond appropriately in the clearance of these small crystals. Previously, our lab has shown that ADPKD cyst lining epithelial cells exhibit increased levels of mTOR and STAT3 activity[6–8]. This same activation of mTOR and STAT3 can be seen following calcium oxalate crystal deposition in both wild-type mice and rats. In addition to the increase in STAT3 and mTOR activity, there is a concomitant increase in tubule dilation. This dilation persists until crystals are no longer detected in kidneys along with a cessation of mTOR and STAT3 activity. Additionally, we demonstrate that the Han:SPRD and pck rat models of PKD exhibit an exacerbated renal phenotype following an increase in kidney microcrystals. Cyst number and cystic index increase following crystal deposition demonstrating that the mechanism of cystogenesis is crystal dependent. The discovery that crystals act as a trigger for cyst formation is an important step in elucidating the causal mechanism of cystogenesis in ADPKD and a critical step in creating effective preventative and palliative strategies.

TABLE OF CONTENTS

LIST OF FIGURES

I. Introduction

Autosomal Dominant Polycystic Kidney Disease

Autosomal dominant polycystic kidney disease (ADPKD) is a slow-onset disease, characterized by the generation of multiple fluid filled cysts within the kidney. Presenting in early adulthood, ADPKD is manageable until the 4th or 5th decade of life when cystic and fibrotic tissue replace normal, healthy tissue leading to renal failure[9]. ADPKD is a monogenic disorder caused by mutations in either the *Pkd1* or *Pkd2* alleles and their respective gene products polycystin-1 or polycystin-2 respectively. Mutations in *Pkd1* account for approximately 85% of cases reported with *Pkd2* mutations comprise the remaining 15% of cases[10]. ADPKD has an extremely high penetrance, and can be caused sporadically affecting between 1:400 and 1:1000 live births world-wide making it the number one life-threatening monogenic disorder.

In addition to the effects of ADPKD on the individual, the societal cost of ADPKD is extremely high due to lost wages and governmental aid for treatment[1]. Research on targeting molecular pathways associated with ADPKD has yielded little return on investment leaving dialysis and kidney transplantation as the only viable alternatives after the onset of end stage renal disease (ESRD). In 2010, 32.9 million Americans began dialysis because of cystic kidney disease. Among the ADPKD patients receiving dialysis, 10% developed ESRD. The annual expenditure for dialysis in the United States currently exceeds $47 billion making alternative treatments fiscally important. The lack of ADPKD treatment options and the cost of dialysis creates an enormous societal cost from the lost earning potential of sufferers along with the loss of tax payer dollars to support healthcare costs for patients[1,11]. Depending

on disease severity, annual spending for advanced stage patients can reach between approximately $30,000-$140,000 for care including dialysis and medication[11].

Focus on the treatment of ADPKD is to preserve renal function for as long possible. Individuals with ADPKD living in the United Kingdom have recently been able to receive the only clinically approved therapy, Tolvaptan. Tolvaptan is a vasopressin antagonist that may help to reduce the progression of ADPKD by decreasing the levels of cyclic-AMP within cysts[12]. Tolvaptan has been used previously for the treatment of hyponatremia and has recently been approved for the treatment of ADPKD. The side effects of increased and frequent urination from Tolvaptan make it difficult for patients to tolerate and there are dangerous contraindications with other drugs, making it far from a treatment of choice or a cure for ADPKD.

The function of the polycystin-1 and polycystin-2 proteins is still poorly understood in ADPKD. Polycystin-1 associates with TSC2, an important regulator of the mTOR pathway. Together, the polycystin-1 and polycystin-2 proteins cooperate to form a calcium channel found on the primary cilium of kidney epithelial cells, allowing luminal fluid flow sensation by increasing intracellular calcium permiability[13].

Homozygous mutations in *Pkd1/2* or autosomal recessive PKD (ARPKD), leads to rapid cyst formation in utero, birth defects and premature death. The loss of heterozygosity in *Pkd1/2* is a hallmark of the disease state and has led to the development of a “two hit” model of cystogenesis. Inactivation of *Pkd1* prior to post-natal day 13 (P13) in mice leads to rapid cyst formation whereas inactivation after P13 only results in cyst formation after 5 months[14]. The slow onset of cystogenesis can be accelerated with renal injury leading to a “*three hit*” model for cyst formation[2,15]. This model has been tested with different kidney injuries including: nephrotoxins, ischemia reperfusion, and, unilateral and partial nephrectomy[3–5,15].

Many other polycystic kidney disorders have been characterized in addition to ADPKD, stemming from the lack of critical polycystin like proteins[16], lack of or dysregulated primary cilia[17], or the dysregulation of planar cell polarity[5]. Trafficking of polycystin-1 to the primary cilia has also been shown to be critical for cyst formation[18].The interface between the PKD disorders appears to be regulation of cell polarity and signaling through the primary cilia as many proteins known to result in PKD are associated in some way with primary cilia or ciliary trafficking[19,20]. Additionally, the loss of the primary cilia has been shown to be critical in the development of PKD following injury[21]. Loss of primary cilia maintenance critically disrupts cellular signaling, planar cell polarity and the localization of the polycystins[19].

The primary cilia associates with a host of proteins needed for control of cell signaling including; proliferation, differentiation, tissue maintenance, cell polarity and proper ciliary maintenance. Loss of any of the trafficking proteins for cilia maintenance results in alteration of cilia integrity or loss of the cilia entirely[17]. The primary cilia are involved in signaling by interacting with the extracellular environment and integrating signals via interacting proteins along the surface of cilium. The cilia act as a mechanosensor and can detect bending from extracellular tension. An example is fluid flow in the tubule lumen. Cilia bending has been shown to be able to activate PC1/2 mediated calcium channel activity that inhibits increases in intracellular cAMP[13]. Mechanical bending of the cilia has also been shown to produce PC1 cleavage of the C-terminal tail leading to p100 mediated gene transcription[22]. Loss of cilia produces a mislocalization of the polycystins and the inability to signal the presence of fluid flow.

Cystogenesis

The *Three Hit Hypothesis* posits that cyst development is believed to be a multifactorial process of mutation and injury, resulting in a futile repair mechanism[2]. The model of cyst development currently accepted by the field is akin to the model for cancer development. The *Three Hit Hypothesis* predicts that *Pkd1* or *Pkd2* mutations alone are not sufficient to promote cyst formation, nor is the loss of heterozygosity[23]. Instead cyst formation results from the accumulation of both genetic and somatic mutations followed by a "third hit" injury to the kidney[2,15]. This model of cystogenesis can explain the slow-progression of cyst formation observed in ADPKD.

The "hits" are a stepwise function leading to the formation of a cyst. The "first hit" is a germ line mutation of the *Pkd1/2* allele. Kidney epithelial cells are still able to function and behave as normal due to the functional redundancy of the second allele of *Pkd1/2*. At some point, a "second hit" occurs to the functional copy of *Pkd1/2*, creating a somatic mutation and a cell that contains two mutated *Pkd1/2* genes. Work done on elucidating the origin of cysts has shown that cysts result from a clonal expansion of a single mutated cell that exhibit unique mutations between cysts[24]. This shows that there was a loss of heterozygosity due to somatic mutation prior to cyst formation. This loss of heterozygosity alone, however, is not sufficient to promote cyst formation as has been demonstrated using an inducible *Pkd1* knockout mouse line[25]. Following this second hit, the kidney appears normal for many months, even with the complete loss of heterozygosity. This could also explain the slow progression of the diseases in humans.

In addition to the germ line and somatic mutations required for cyst formation, it has been shown that both the timing of the mutations and the application of the "third hit" injury are necessary for rapid cyst formation[23]. Application of an injury results in rapid cyst

formation following the loss of *Pkd1/2* in several studies[3–5,15,26,27]. In animal models mutation of *Pkd1/2* is embryonic lethal due to the role of polycystin-1/2 in organogenesis during development[10]. To circumvent the lethality of PC1/2 mutation, animal models used to study ADPKD utilize inducible knockouts or animals with variegated expression of PC1/2 to study their effects on cyst formation[3,4,23]. Both complete and partial inactivation of PC1 has been shown to play a critical role in cyst development[28]. Animals that have PC1 inactivated at embryonic day 13 (E13), show rapid cyst development in utero whereas after P28, analogous to a young adult human, there was no cyst formation for more than 12 weeks. If there was an injury to the kidney however, then cyst formation occurred rapidly[23,25]. The mouse kidney is fully developed after 1 month (P28) implicating cystogenesis is facilitated by mitogenic signaling in the developing animal. In support of this, PC1 has been shown to be a direct regulator of the mTOR signaling pathway[29] and when looking at ADPKD kidneys in mice, we can see that there is an upregulation of Src and mTOR signaling[6–8,30]. These signaling pathways for growth and proliferation are highly expressed in the developing animal until maturity and may account for the lack of cyst development after the developmental cutoff. Following injury there is an increase in cell proliferation and the re-activation of the mTOR and Src signaling pathways. Injury induced cyst formation is most likely caused by the initiation of cellular repair in response to insult and the upregulation of these mitogenic signaling pathways from the repair process[27]. Injuries that trigger cystogenesis have come in the form of nephrotoxic compounds[4], partial and total unilateral nephrectomy[21], and ischemia reperfusion[3]. Each of these injuries to the kidney creates an environment where the kidney must undergo a process of repair and proliferation in response to insult[15].

The *Three Hit* model of cystogenesis hypothesizes the defect in ADPKD to be associated with a futile repair response following injury[2]. While experimental treatments have demonstrated that the ADPKD kidney's response to injury is maladapted, the sources of experimental injury are not likely to account for the cause of human ADPKD cystogenesis. ADPKD is a slow onset disease, implying that the triggering third hit is an environmental factor. The failure of the experimental approaches thus far is that they have not been able to show what the endogenous trigger for injury might be. While various forms of kidney injury are sufficient to promote cystogenesis in the context of a *Pkd1/2* null animal, none of these techniques point to an endogenous trigger. What that trigger may be has been elusive to this point, but may be a potential therapeutic target for intervention.

My research aims to uncover an as of yet, unrecognized mechanism for the clearance of tubular obstruction and a form of kidney injury. I propose that tubular injury caused by the interaction between the tubule lumen and microcrystals act as a third hit that causes disease progression in PKD mutant cells. Crystal obstruction causes the cessation of fluid flow and the production of cellular intermediates such as reactive oxygen species and inflammatory cytokines. This process leads to the activation of the mTOR and STAT3 signaling pathways along with tubule dilatation (Fig. 1, 3B,C,E). In normal kidneys, this process stops once the tubule is cleared of the crystals but will continue to grow and form a cyst in a polycystic kidney.

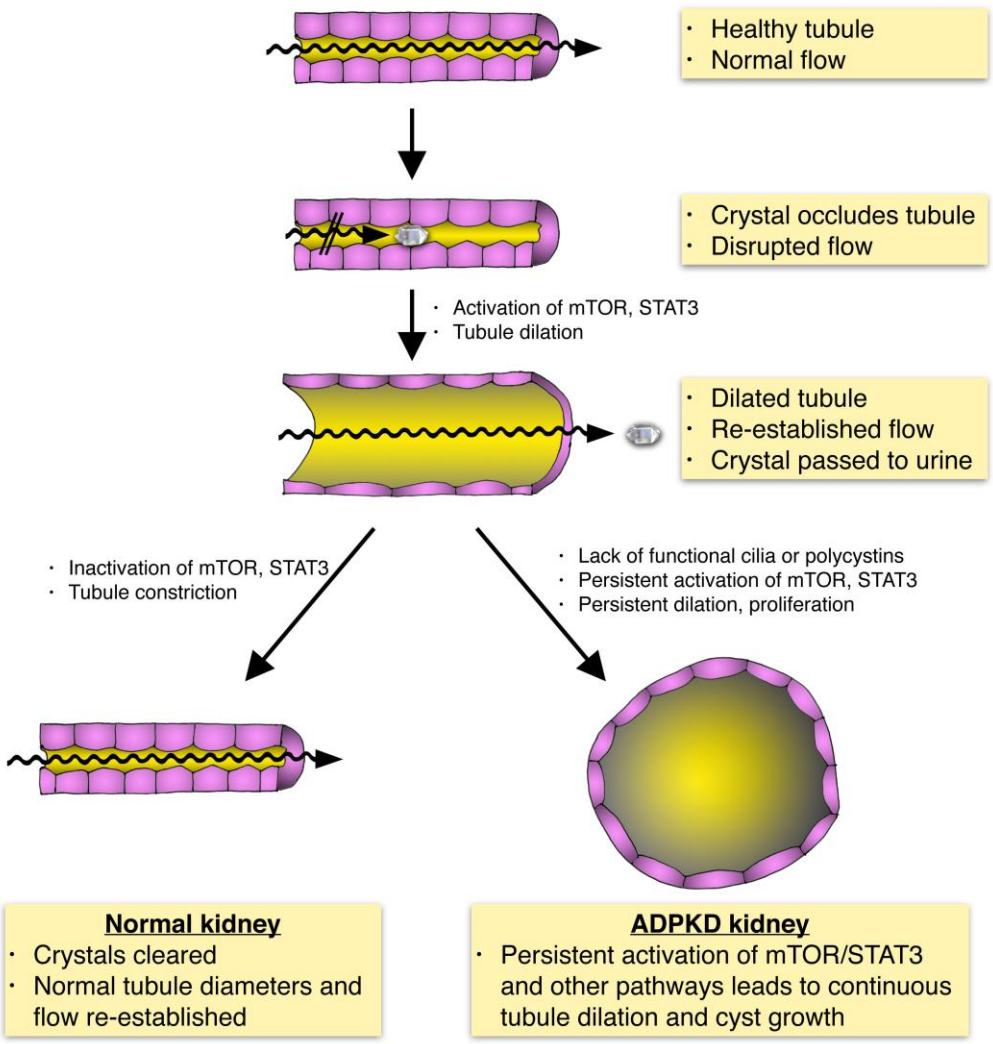

Figure 1: Model of microcrystal induced cystogenesis: Interaction between microcrystals and the tubule lumen cause the tubule to dilate in response to occlusion. Dilatation occurs allowing for the crystal to be flushed out. Under normal circumstances the tubule returns to normal diameter but in PKD kidney this effect persists, leading to a cyst.

Cyst Structure and Function

Cysts are a fluid filled monolayer created from the epithelial layer of cells in the tubule lumen of the kidney (Fig. 1). Cysts have been shown to be created from the clonal expansion[24] of mutant cells along any tubule segment of the nephron, with the origin of which depending on the model being studied. The lumen of the cysts contains a host of secreted factors including cytokines, secondary messengers and immunoglobins[31]. The

increase in cyst size and number leads to a hypoxic environment as the renal parenchyma is replaced with fibrotic tissue as cysts proliferate and expand.

The change in kidney architecture leads to a shift in cellular metabolism towards aerobic glycolysis similar to the Warburg effect observed in hypoxic tumors[32]. Treatment with the glycolysis inhibitor 2-deoxyglucose, has been shown to be effective in ameliorating the size of cysts in rodent models[32]. Sans metastasis, the similarities between cysts and cancer are striking as both cysts and cancerous tumors are in hypoxic environments, formed by multiple gene mutations, exhibit an increase in mitogenic and autocrine signaling, are proliferative, and change their metabolism to allow for continuous growth.

The epithelial cells lining cysts exhibit strong proliferative signals. Our lab has studied the effect of the mTOR pathway as a treatment for PKD, as cysts show increased levels of phospho-S6 in all models of PKD including human ADPKD[7,8]. The role of mTOR and cyst growth is demonstrated by inhibition of the mTOR pathway with rapamycin as an effective treatment in the BPK mouse and the Han:SPRD rat[8,33] model of PKD. Treatment with rapamycin or rapalogs has been shown to slow the disease progression in animals, but unfortunately was ineffective in human trials and may be potentially dangerous for long-term application[34]. Cyst fluid is highly enriched in cAMP leading to the assumption that the effect of vasopressin antagonism may provide relief to cyst development[35]. Altering cAMP signaling with the vasopressin antagonist Tolvapton[12] is modestly effective, but not without side effects such as polyuria and nocturia that lead to a high rate of non-compliance. Thus, it is important to identify additional, druggable targets to halt or slow progression of the disease.

Animal Models of PKD

The varying ways in which PKD can manifest has produced several orthologous and non-orthologous animal models that are utilized to study PKD. Prior to the discovery and cloning of the *Pkd1* gene into mouse models, several rat models had been studied for their sporadic PKD phenotypes. For my research, I utilized the non-orthologous Hannover:Sprague-Dawley and pck rats. The cystic disease from these animals results from mutations in the proteins samcystin and fibrocystin respectively[16,36]. These models of PKD have been well established and are widely used for the study of ADPKD.

An extensive list of animal models has been developed to study ADPKD. These include mutations in *Pkd1*, *Pkd2*, cilia trafficking proteins, polycystin homologs and other genes involved in more rare forms of PKD and nephronophthisis[10,18,18]. The animals that I have utilized to perform my research are discussed in more detail below.

Pck Rat

The pck rat is a non-orthologous model of PKD that exhibits extra renal manifestations in the liver and form cysts in the thin ascending limb of Henle, cortical collecting ducts and distal tubules which make its phenotype more similar to human PKD[37]. The mutation associated with the pck rat is the polycystin like protein fibrocystin, encoded by the *Pkhd1* gene. A significant difference with the pck rat phenotype is autosomal recessiveness rather than autosomal dominanance[38]. This mode of inheritance and the gene product fibrocystin's localization to primary cilia make the pck rat an incomplete model of ADPKD. Fibrocystin localizes to primary cilia and associates with the NPHP family of proteins. The NPHP proteins are associated with nephronophthisis, a recessive PKD disease. This association and the recessive inheritance make the pck rat more related to a ciliary disease model of PKD.

Han:SPRD

The Hannover rat is a non-orthologous model of ADPKD that was discovered in a colony of Sprague Dawley rats in 1989[39]. These animals are carried as heterozygous mutants, with males exhibiting a more severe cystic phenotype than females[40]. Homozygous male animals do not survive past 3 weeks of age with kidneys so large they begin to affect breathing and movement. Heterozygous males develop cysts rapidly until 8 weeks of age and then begin to lose kidney function for several months until reaching ESRD. Interestingly, females do not suffer from the same level of PKD as males. This difference in between the sexes has correlates in human ADPKD, as males are observed to suffer from more severe forms of the disease than do their female counterparts. This difference in the PKD phenotype was utilized in our research for designing experiments to assess the effects of treatments between male and female rats treated with ethylene glycol and their cystogenic response. It is worth mentioning that female rats are not susceptible to the effects of ethylene glycol administration unlike the male rats, which readily produce calcium oxalate crystals in response to ethylene glycol.

My research has utilized both of the described animal models to study PKD. Despite their limitations both have proven useful. In Chapter II, I present my results using both rat models of PKD to study the effects of crystal deposition and the effects of crystals on cystogenesis. In Chapter IV I use the Han rat to study the possibility that a ketogenic diet may be effective at treating ADPKD.

II.

Renal Crystal Deposition Leads to Tubule Dilation to Facilitate Excretion in Normal Kidneys but Promotes Cystogenesis in Polycystic Kidney Disease

This chapter is in preparation for submission with the following co-authors;

Mina Rezaei[1], Louis Lin[1], Caroline Broderick[1],

Benjamin Cowley[2], Vicente Torres[3], Saeed Khan[4], Thomas Weimbs[1]*

[1]University of California Santa Barbara, Department of Molecular, Cellular, and Developmental Biology, and Neuroscience Research Institute;

[2]University of Oklahoma Health Sciences Center, Department of Medicine;

[4]Mayo Clinic College of Medicine, Division of Nephrology;

[4]University of Florida, Department of Pathology

Abstract

ADPKD is a progressive disease characterized by the accumulation of fluid-filled cysts, slowly replacing healthy tissue progressing to renal failure. Individuals with ADPKD suffer from many renal pathologies including nephrolithiasis. Throughout evolutionary time the kidney has developed mechanisms to allow for small occluding bodies to be passed without incident. We hypothesize that tubular expansion and cyst formation is an aberrant activation of this endogenous pathway. Administration of sodium oxalate via intraperitoneal injection leads to calcium oxalate crystal deposition inside kidney tubules and subsequent activation of the mTOR, Src and STAT3 pathways and concomitant tubule expansion in wild type rats and mice. We demonstrate crystal dependent cystogenesis in both the Han:SPRD and pck rat. The discovery of microcrystals as the endogenous trigger for cyst formation allows for an avenue of therapeutic intervention, potentially without the use of dangerous or unsustainable drug treatments.

A. Introduction

ADPKD is a common, life-threatening genetic disease that causes immense human suffering and places a significant economic burden to the health care system[1]. Progressive renal cyst growth leads to the deterioration of normal renal parenchyma, and approximately 50% of patients will require dialysis or kidney transplantation in adulthood[9]. No approved treatment to slow or halt disease progression is available in the US. Recently, a vasopressin receptor antagonist, Tolvaptan, has been approved for ADPKD in other countries but the utility of this drug may be limited by significant adverse effects, potential liver toxicity and high costs[41]. There is an urgent need for effective and safe treatment options for ADPKD.

ADPKD is caused by mutations in either the *Pkd1* or *Pkd2* gene. Numerous functions for the respective gene products, polycystin-1 (PC1) and polycystin-2 (PC2), have been identified, but the actual role of the polycystins in the kidney remains to be determined[42]. The rate of disease progression in ADPKD exhibits high inter- and intra-familial variability, suggesting involvement of modifier genes and/or environmental factors[43–47], yet none have been clearly identified. If an environmental factor influences disease progression it would be of utmost importance to identify it so that it can be controlled. Support for a role of environmental factors as determinants of disease progression in ADPKD has come from genetic mouse experiments that culminated in the widely accepted “third hit” model of cystogenesis[2]. In this model three events must occur to trigger the formation of individual cysts in ADPKD: the “first hit” is a germline mutation in the *Pkd1* or *Pkd2* gene; the “second hit” is a random somatic mutation in a single

tubule cell that affects the other *Pkd1/Pkd2* allele; the "third hit" is an insult to the affected kidney such as ischemic or toxic damage that triggers a repair response. Indeed, elimination of both *Pkd1* alleles in mature mouse kidneys alone does not lead to cyst growth for many months [14]. However, subsequent renal injury in such mice – or similarly pre-conditioned mice - will trigger rapid cyst growth[2–5,15,21]. In human ADPKD, new cysts are thought to arise throughout life[48]. Since most "second hits" (somatic mutations) in ADPKD patients presumably occur long after kidney maturation, it is likely that subsequent "third hits" (damage/repair) are also required for cystogenesis in humans. However, ischemic or toxic kidney damage are infrequent events in humans and unlikely to explain the relatively constant progression of ADPKD although it is possible that subclinical levels of such injuries may play a role. We therefore hypothesized that a much more prevalent, and clinically relevant, mechanism may drive disease progression as a "third hit" trigger, and considered tubule occlusion or injury by sporadically lodged microcrystals.

Kidneys are constantly challenged by super-saturated solutes – such as calcium oxalate (CaOx), calcium phosphate (CaP), uric acid and others – present in the urinary filtrate that may precipitate while passing through the tubular system. While millions of microscopic crystals may form in human kidneys daily, most are excreted safely with the urine[49,50]. Diets and numerous pathologies greatly influence the range of crystal burden that the kidneys experience. Up to a quarter of fresh urines from normal subjects exhibit overt crystalluria[51] without immediate detriment to normal kidneys. Innate mechanisms prevent excessive growth and retention of crystals within the luminal space. Otherwise, tubules

would rapidly become occluded and renal function would seize. Protective mechanisms include renal regulators of crystal nucleation and growth such as osteopontin, nephrocalcin and Tamm-Horsfall Protein (THP)[50]. If crystals do become lodged in renal tubules, e.g. due to fast growth or aggregation, it can lead to nephrolithiasis. The fate of such lodged microcrystals is poorly understood but the main proposed mechanism for their excretion is that they cross the epithelium into the interstitial space where they would either be resorbed or lead to the formation of kidney stones[52]. In humans, 70-80% of all kidney stones are composed of CaOx indicating that oxalate provides a particular challenge.

Several correlative observations may support a link between ADPKD progression and renal crystal burden. Symptomatic nephrolithiasis is common (up to 20-28%) among ADPKD patients[53–56]. Importantly, ADPKD patients with nephrolithiasis exhibit more severe polycystic kidney disease than those without[57,58]. Hyperoxaluria was found in 18% of ADPKD patients that are associated with nephrolithiasis suggesting the presence of CaOx crystals in some patients[57]. ADPKD patients also have high incidences of clinical gout (24%) and hyperuricemia (>60%)[57,58], conditions that are associated with uric acid crystal formation in the kidneys. Elevated urinary uric acid levels are significantly correlated with faster disease progression in ADPKD[59]. Interestingly, ADPKD progresses more rapidly in males than females[43]. Likewise, male rats are naturally more prone to CaOx nephrolithiasis compared to female rats[60]. In the Han:SPRD rat model of ADPKD, male animals are affected more severely than females[40,61]. This dual gender bias in humans and rats may be consistent with a role of crystal deposition in accelerating ADPKD progression.

We have investigated the possible role of renal crystal deposition in affecting the rate of progression of PKD. In the process, we uncovered a previously unrecognized mechanism that facilitates the passage of microcrystals by tubule dilation. We report here that acute or chronic induction of CaOx nephrolithiasis in normal rats and mice leads to rapid activation of mTOR and Src/STAT3 signaling pathways accompanied by rapid dilation of tubule diameters along the entire tubular and collecting duct system. The same signaling pathways are known to be activated in ADPKD and contribute to renal cyst growth. After acute oxalate treatment, in approximately 7 days, CaOx crystals are cleared via the luminal space, these signaling pathways are inactivated and tubule diameters return to normal. Inhibition of mTOR by treatment with rapamycin significantly blocks tubule dilation and leads to renal accumulation of large CaOx crystal aggregates. These results suggest that tubule dilation is a purposeful mechanism in response to lodged microcrystals with the apparent goal of "flushing out" such crystals. This mechanism has not previously been recognized. Furthermore, we show that chronic oxalate exposure leads to tubular CaOx crystal deposition in male, but not female, animals of the Han:SPRD rat model of polycystic kidney disease. This leads to increased cystogenesis and significant worsening of disease progression in male, but not female, animals. Similarly, we report that a high phosphorous diet causes tubular CaP crystal deposition in the PCK rat model of polycystic kidney disease and leads to accelerated disease progression. Altogether, these results suggest a model in which tubular crystal deposition normally triggers a protective mechanism leading to temporary tubule dilation. In polycystic kidney disease, this mechanism could act as a "third hit" trigger that causes such dilated tubules to

"overshoot" to form cysts. If this mechanism affects the rate of disease progression in human ADPKD then it may consequently be possible to treat patients with relatively simple and well-established interventions known to reduce renal crystal formation in nephrolithiasis patients. These could include dietary changes, increased water intake and treatment with citrate as a calcium chelator. Intriguingly, increased water intake[62,63] and citrate treatment[64–66], respectively, have already been shown to be effective in rat models of PKD[66] but the underlying mechanisms have remained elusive and it has not previously been considered that an effective reduction of renal crystal burden may be involved.

B. Results

Chronic CaOx nephrolithiasis leads to tubule dilation and activation of PKD-associated signaling pathways.

To examine whether CaOx crystal deposition may lead to activation of PKD-associated signaling pathways, a well-established mouse model of chronic CaOx nephrolithiasis was utilized. Animals deficient in the renal sodium-phosphate cotransporter Npt2a are calciuric and form CaOx crystal deposits in their kidneys when fed either hydroxy-proline or glyoxylate as metabolic precursors of oxalate[67,68]. As expected, treated animals exhibit numerous luminal CaOx crystal deposits visible by polarized light microscopy after 28 days (Fig. 2A). Significant tubule diameter dilation is very apparent throughout the renal parenchyma (Fig. 2A). Analysis with segment-specific markers revealed that proximal tubules (LTL), connecting tubules (calbindin D28k) and collecting ducts (DBA) all exhibit dilation (Fig. 2B). Strikingly, dilated tubules are strongly positive for phosphorylated S6 (pS6) a downstream effector of the mTOR signaling pathway

indicating that mTOR is activated in these cells (Fig. 2C). In contrast, adjacent undilated tubules do not exhibit mTOR activation (Fig. 2C). Similarly, dilated tubules are also strongly positive for active, nuclear, tyrosine-phosphorylated STAT3 (Fig. 2C). Both mTOR and STAT3 have previously been shown to be activated in cyst-lining cells in human ADPKD and various rodent models of PKD, and to be drivers of renal cyst growth[6–8,69–71]. For comparison, kidneys from the Bpk mouse model of PKD were analyzed side-by-side and showed a degree of mTOR and STAT3 activation similar to that induced by nephrolithiasis (Fig. 2C). Dilated tubules also frequently contained Ki67-positive cells (Fig. 2D, E) indicating that chronic nephrolithiasis induces a proliferative response.

Rapid activation of PKD-associated signaling pathways and tubule dilation in acute CaOx nephrolithiasis.

To test whether tubule dilation and activation of PKD-associated signaling pathways are slow or fast responses to CaOx crystal deposition wild-type mice were treated acutely by a single intraperitoneal injection of sodium oxalate and analyzed at different time points thereafter. For unknown reasons, mice are relatively resistant to the formation of renal CaOx deposits[67,68]. A high dose of oxalate (0.7 mg/kg) was initially used to induce acute nephrolithiasis which led to rapid, abundant crystal deposition (Fig. 3A) appearing to be exclusively luminal (Fig. 3B). This coincided with rapid activation of mTOR and STAT3 at 3 hours and peaking at 1 day following treatment (Fig. 3C).

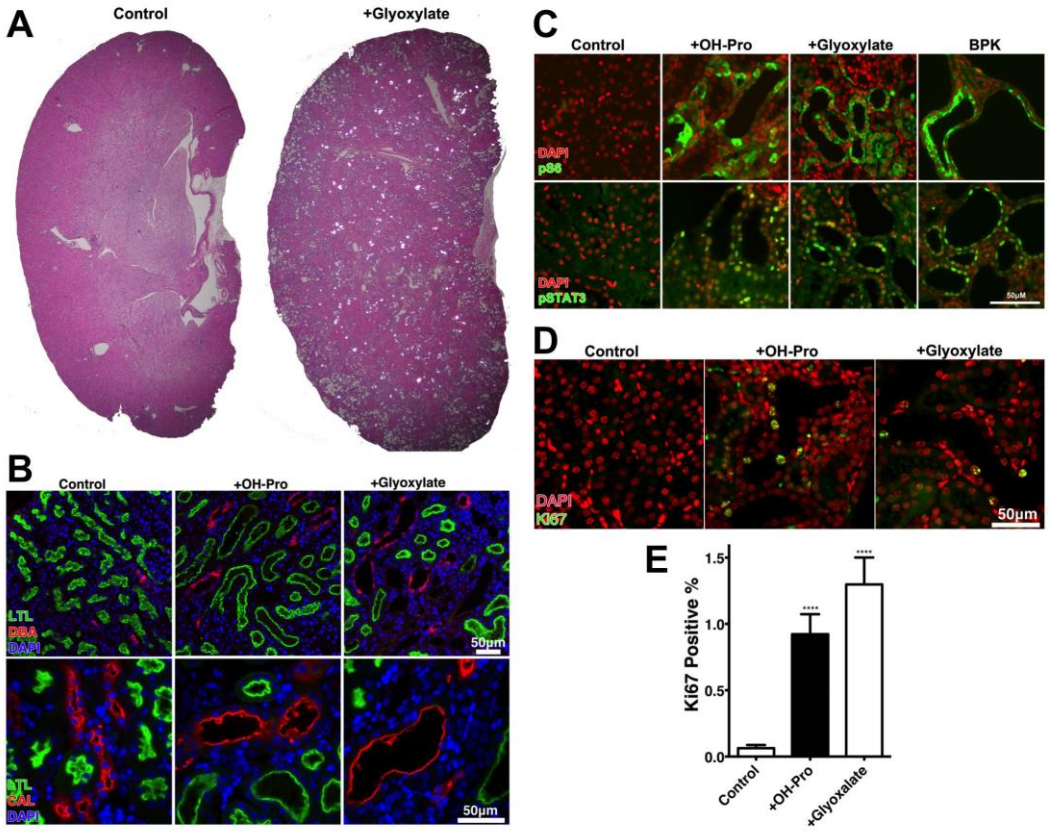

Figure 2: Glyoxalate treated Npt-KO Mice show tubule dilation and activation of ADPKD related pathways

A.) H and E Stain: Sections of kidneys from glyoxylate treated Npt2a -/- mice under polarizing microscopy. **B.)** Segment specific staining of glyoxylate or hydroxy proline treated Npt2a -/- mice of LTL, DBA and Calbindin. **C.)** mTOR activity marker phospho-S6$^{S235/236}$ and phospho-STAT3^{Y705} by immunofluorescence microscopy in the kidneys of treated Npt2a -/- mice. BPK mouse used as positive control. **D.)** Immunostaining for Ki67 in treated Npt2a -/- mice. **E.)** Quantification of Ki67 positive cells of the total number of DAPI stained nuclei with either glyoxylate or hydroxyl proline treatment. (Control n=3, n=3 for glyoxylate and n=2 for HP) ****= (>P=0.001) Error bars represent SD.

High-dose oxalate treatment led to significant renal impairment and frequent death due to renal failure after several days.

To induce a low, recoverable level of crystal burden we next administered via IP injection a low dose of oxalate (0.3 mg/kg) which resulted in CaOx crystal

deposition observed as early as 6 hours after injection, peaking at 24 hours, with most crystals excreted by 3 days (Fig. 3D). Abundant CaOx crystals are detectable in urine from 6 hours until 3 days after injection (data not shown). Tubule dilation can be seen as early as 1 day and peaking at 3 days (Fig. 3D). By seven days post injection all CaOx crystals are eliminated and tubule diameters return to normal (Fig. 3D). At all time points that CaOx crystals are visible they are found nearly exclusively in tubule lumens suggesting that the bulk of crystals are excreted with the urine via the luminal space (Fig. 3D). Dilated tubules exhibit activation of mTOR and STAT3 as early as 1 day after oxalate administration indicating that this is an early event coinciding with the process of tubule dilation (Fig. 3E). Mice survived this low-dose oxalate treatment and appeared to completely recover. However, some animals failed to form renal CaOx crystals consistent with the known resistance of mice to CaOx nephrolithiasis.

Calcium Oxalate Crystals Activates ADPKD Pathways and Promotes Dilatation in Wild-Type Rats

To be able to quantify responses more accurately we next investigated the response to CaOx crystal deposition in a more robust experimental system. Rats are commonly used to experimentally induce CaOx nephrolithiasis because they are much more prone than mice to forming CaOx crystals following oxalate administration, are more resilient after crystal deposition and recover more consistently[72–74]. A single injection of sodium oxalate in rats again led to rapid renal CaOx crystal deposition within 6 hours accompanied by fast tubule dilation (Fig. 4A). After seven days, all crystals were cleared. Analysis using segment-specific markers revealed that all investigated nephron segments undergo dilation,

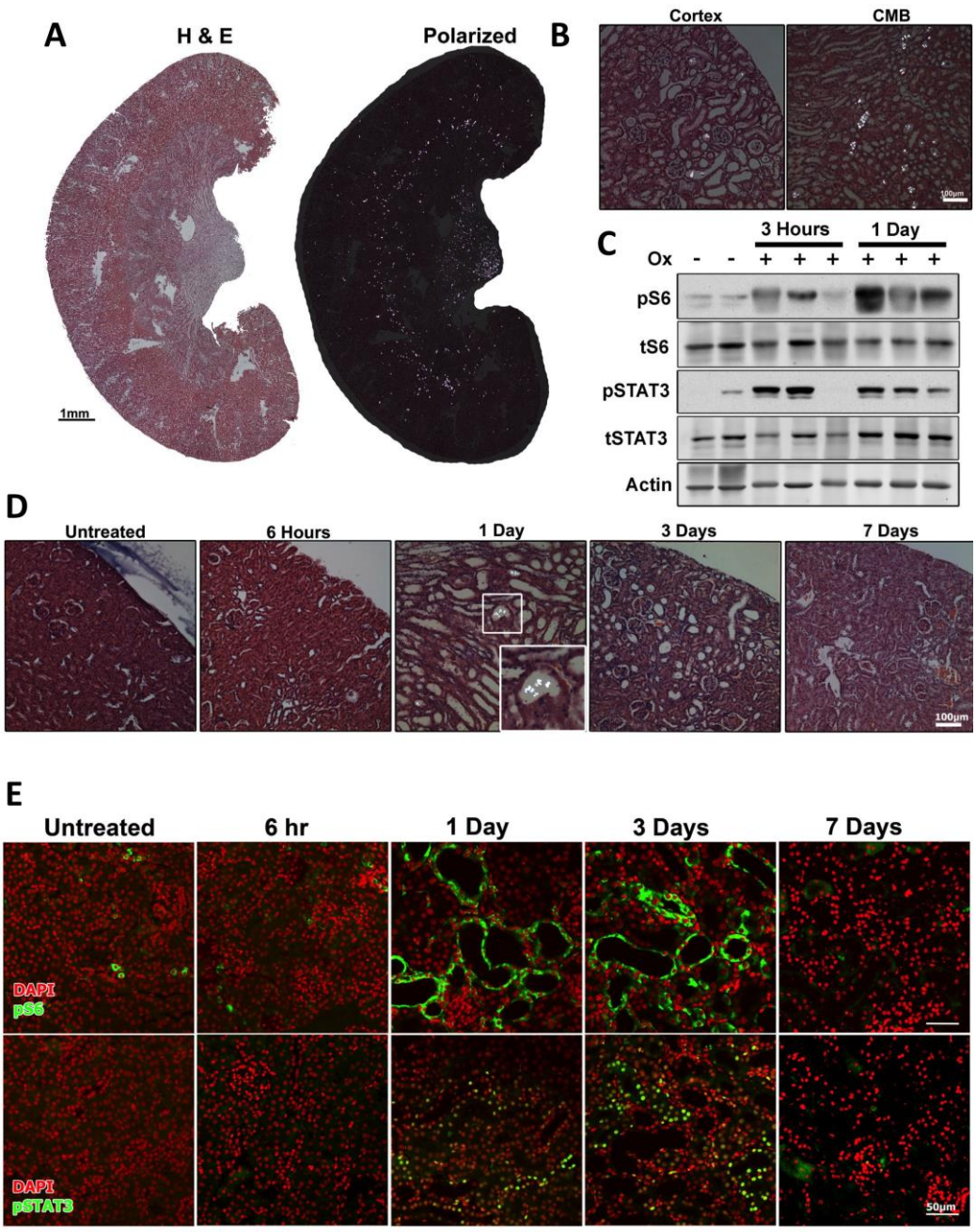

Figure 3: Effect of sodium oxalate treatment on wild-type C57/B6 mice.
A.) Whole kidney polarized microscopy image of oxalate treated (7mg/100g NaOX) mice. **B.)** High magnification polarized image of 1 day treated mouse of cortex and corticomedullary boundary (CMB). **C.)** Immunoblotting from wild type mouse kidneys of pS6 and pSTAT3 3 hours (n=4) and 1 day (n=9) post 7mg/100g oxalate treatment. **D.)** Polarized images of oxalate treated mice (3mg/100g NaOX) 6 hours (n=4), 1 day (n=12), 3 days (n=8) and 7 days (n=13) post treatment. **E.)** Immunofluorescence staining of phospho-S6$^{S235/236}$ and phospho-STAT3^{Y705}in NaOX (3mg/100g) treated mice.

namely proximal tubules, the thick ascending limb, connecting tubules and collecting ducts (Fig. 4B). Quantification of the tubule outer diameters and the lumen diameters revealed that both parameters increased, peaking at day 3 and largely returned to normal by day 7 (Figs. 4C-F). The tubule diameter increase is accompanied by a decrease in cell height (Fig.4G). mTOR and Src/STAT3 signaling were activated in dilated tubules at six hours following injection, reaching a peak at three days (Fig 4H, I). Proliferation was observed to begin as early as 6 hours following oxalate administration and peaking at 3 days (Fig. 4J, K). A non-significant increase in the number of apoptotic tubule cells was observed (Fig. 4L) indicating that this level of crystal burden does not cause extensive cell death.

Altogether, these results indicate that both mice and rats respond to renal CaOx crystal deposition by rapidly activating mTOR and STAT3 signaling, dilating tubule diameters throughout the nephron, initiating a proliferative response, and clearing crystals via the luminal space for urinary excretion.

mTOR Inhibition blunts tubule dilation and impairs crystal excretion.

Next, we investigated whether mTOR activation is necessary for the dilation of tubules in response to lodged CaOx crystals. Rats were treated with rapamycin to inhibit mTOR, followed by acute oxalate challenge. As shown in Fig. 5A,B, rapamycin treatment prevents mTOR activation as anticipated in Fig. 1. mTOR inhibition did not prevent the activation of Src and STAT3 (Fig. 5A,B) indicating that these pathways are not downstream of mTOR. Rapamycin treatment inhibited, but did not fully suppress, proliferation as measured by Ki-67 (Fig. 5C, Supplemental Fig. 2).

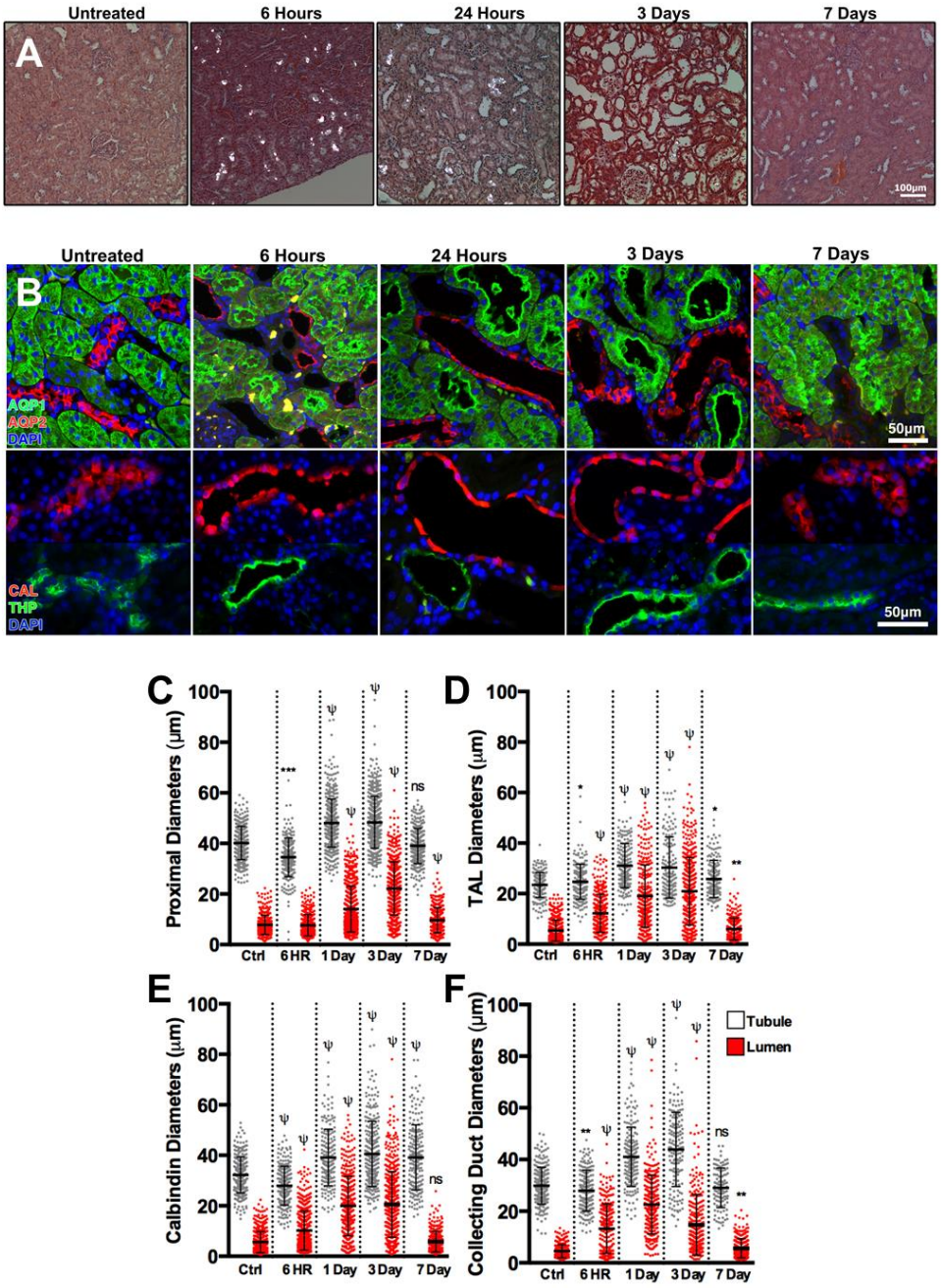

Figure 4: Acute oxalate treatment causes tubule dilation and PKD related pathway activation in wild-type Sprague-Dawley rats

A.) Polarized microscopy images of animals treated with 7mg/100g NaOx after 6 (n=5), 24 hours (n=5), 3 day (n=5) and 7 days (n=3) respectively. **B.)** Segment specific immunostaining of kidney sections; collecting ducts (AQP2), proximal tubules (AQP1), connecting tubules (Calbindin D28K), and thin ascending loop of Henle (Tam-Horsfall Protein) from treated rats. **C-F.)** Measurements of lumen and tubule diameters of AQP1 (C), THP (D), Calbindin (E) and AQP2 (F) segment specific markers.

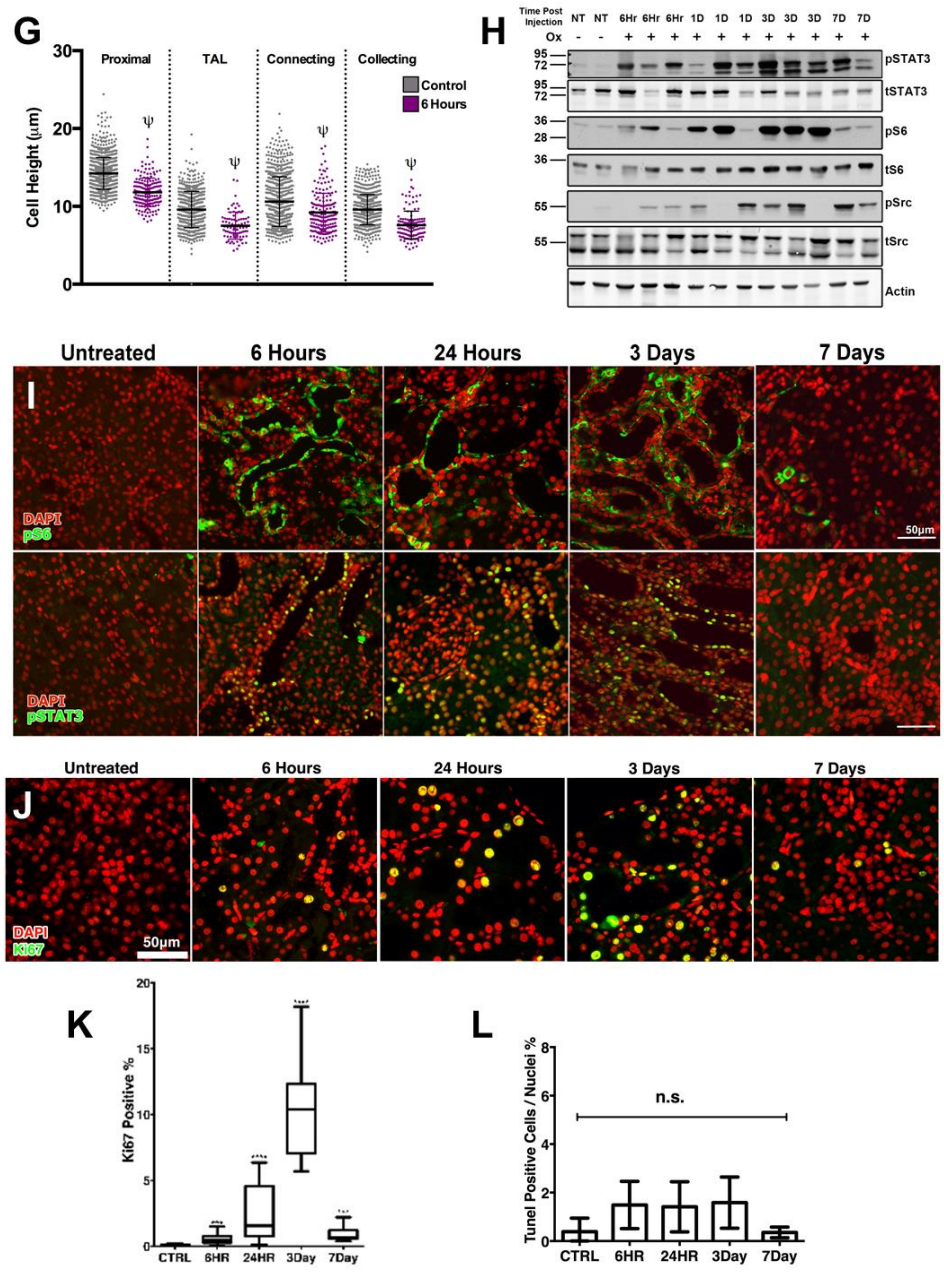

Figure 4: (continued) G.) Cell height measurements from all segments in C-F at 6 hours following treatment. **H.) I**mmunoblotting of total kidney lysates from treated rats**. I.)** Immunofluorescence staining of treated kidneys for phospho-S6$^{S235/236}$ and phospho-STAT3^{Y705} 6 hours, 1 day, 3 days and 7 days after injection. **J.)** Ki67 immunostaining of treated rat kidney sections. **K.)** Quantification of Ki67 positive from J. **L.)** Control and treated rats was evaluated for the presence of apoptotic cells by counting the TUNEL positive cells in each field and normalizing them to the number of nuclei in each field. Error bars represent SD, ψ= (>P=0.0001)

Remarkably, mTOR inhibition blunted the extent of tubule dilation after oxalate challenge (Fig. 5D).

Eventually, all investigated tubule segments were able to dilate in rapamycin-treated animals but to a diminished degree (Fig. 5E) suggesting that mTOR activity is at least partially required for tubule dilation.

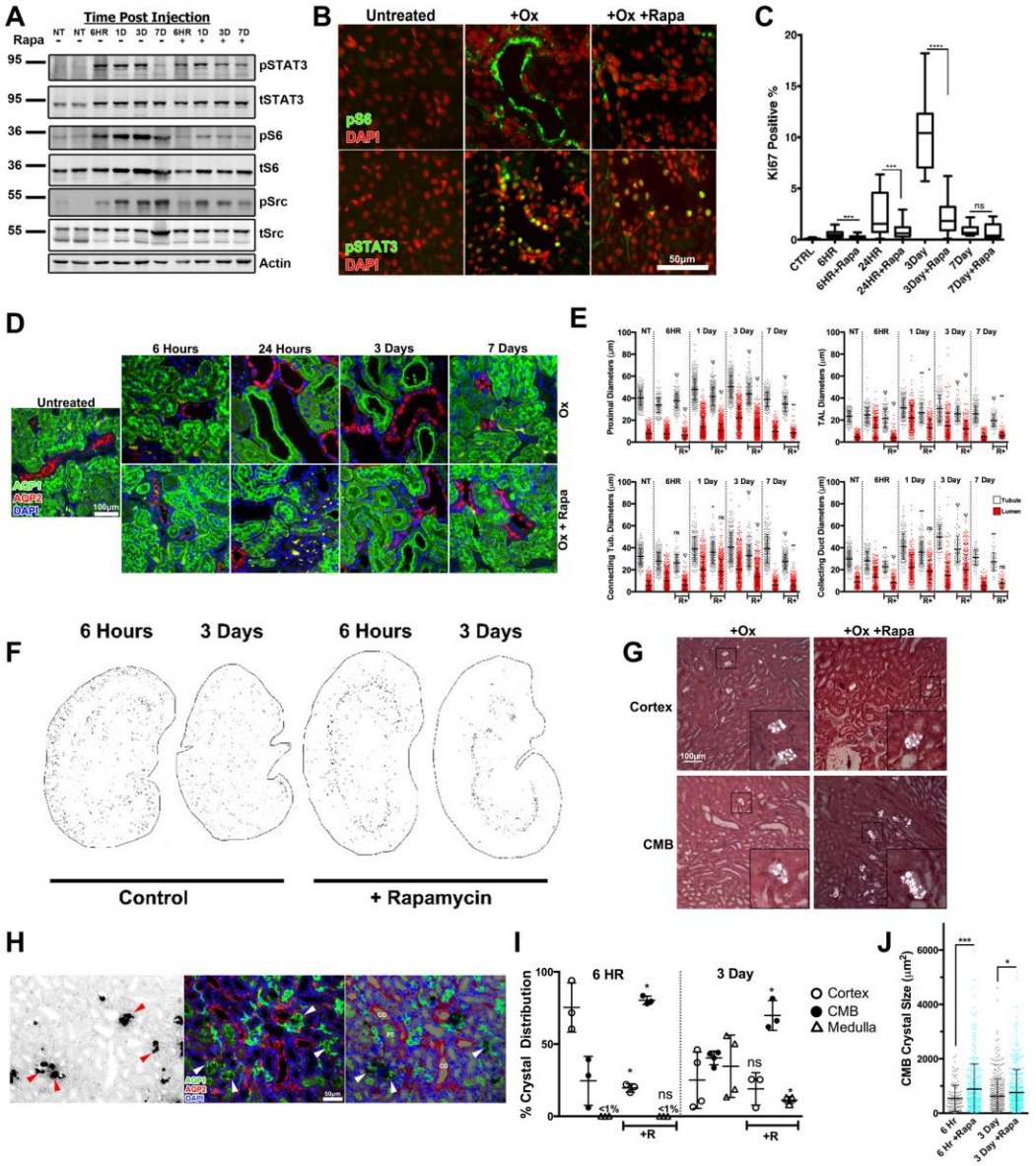

Figure 5: Legend on page 16.

mTOR inhibition led to the striking accumulation of large aggregates of CaOx crystals in tubules located in a distinct band at the corticomedullary boundary (Fig. 5F-H). Immuno-staining with segment specific markers demonstrated that these clusters of CaOx crystals primarily accumulate in the lumens of the thin descending limb of Henle and the preceding segment of the proximal tubule (Fig. 5H). Crystal aggregates are still prominently observed at this border in rapamycin-treated animals at 3 days after treatment (Fig. 5F, I). During this course, crystals are markedly depleted in the renal cortex in rapamycin-treated animals vs. control animals (Fig. 5F, I). These results suggest that mTOR inhibition leads to inhibition of tubule dilation, which creates a "bottleneck" at the point of the nephron that naturally exhibits the smallest lumen diameter, the thin descending limb of Henle. This leads to accumulation of CaOx crystals at this location, which, in turn, prevents the efficient transport of crystals back towards the distal convoluted tubule and the collecting ducts in the renal cortex.

Figure 5: Rapamycin diminishes effect of oxalate treatment on wild type Sprague Dawley rats by inhibiting mTOR pathway
A.) Immunoblotting of NaOX treated rat's kidney lysates. **B.)** Immunostaining of SPRD rats 6 hours after treatment with NaOx, with or without rapamycin pretreatment. **C.)** Quantification of Ki67 positive cells in NaOx and rapamycin treated rats. **D.)** Immunostaining of kidney sections following oxalate treatment, including collecting ducts, proximal tubules by staining with AQP1 and AQP2 respectively **E.)** Measurement of tubular and lumen diameters in oxalate treated rats after rapamycin treatment. ψ= (>P=.0001) **F.)** Polarized images of whole kidneys after 6 hours and 3 days following oxalate treatment **G.)** High magnification polarized images showing oxalate crystal aggregates 6 hours following oxalate treatment with and without rapamycin. CMB=corticomedullary boundary **H.)** Pizzolato staining together with segment specific marker in rapamycin treated rats. Arrows denote crystal location. **I.)** Quantification of deposited crystals in oxalate treated rats 6 hours and 3 days after oxalate treatment with and without rapamycin. **J.)** Quantification of crystal size in oxalate treated rats with and without rapamycin. Error bars represent SD

Altogether, these findings suggest that tubule dilation is a purposeful response to lodged renal crystals, that PKD-related signaling pathways are involved in this process, and that inhibition of this system leads to inefficient clearance of crystals. To our knowledge, this mechanism of crystal clearance has not previously been reported.

CaOx crystal burden leads to increased disease severity in the Han:SPRD rat model of polycystic kidney disease.

We hypothesized that renal crystal deposition may accelerate disease progression of polycystic kidney disease. To investigate this possibility we chose the well-characterized Han:SPRD (Cy/+) rat model of PKD[30,31] because: (a) as a rat model, these animals are more susceptible to CaOx nephrolithiasis than mice; (b) this is a slowly progressive model which may allow for the possibility that disease progression could be accelerated; and (c) male, heterozygous (Cy/+) animals in this model exhibit more severe disease progression than female Cy/+ animals which would be consistent with the known propensity of male rats to be more susceptible to renal CaOx crystal deposition than female rats. Animals were treated from 3-8 weeks of age with 0.75% ethylene glycol in the drinking water (Fig. 6A) for exposure to a chronic burden of CaOx crystals.

Ethylene glycol is metabolized to oxalate leading to hyperoxaluria, and this treatment has previously been shown to lead to CaOx nephrolithiasis in male but not female rats[52,75,76]. Numerous CaOx crystals are readily detectable in lumens of cysts and dilated tubules in male Cy/+ rats but not in female Cy/+ rats (Fig. 6B). Remarkably, male Cy/+ rats treated with ethylene glycol exhibit significantly increased renal cystic disease as compared to untreated animals (Fig. 6B). In

contrast, disease progression is unaffected by ethylene glycol treatment in female Cy/+ rats. The two-kidney weight/body weight ratio (Fig. 6C) and renal cystic area (Fig. 6D) are both significantly increased in ethylene glycol-treated male Cy/+ rats vs. controls. A significant increase in cyst number (Fig. 6E), but not average cyst size (Fig. 6F), is also observed suggesting that the increased disease severity is largely due to an increase in cystogenesis.

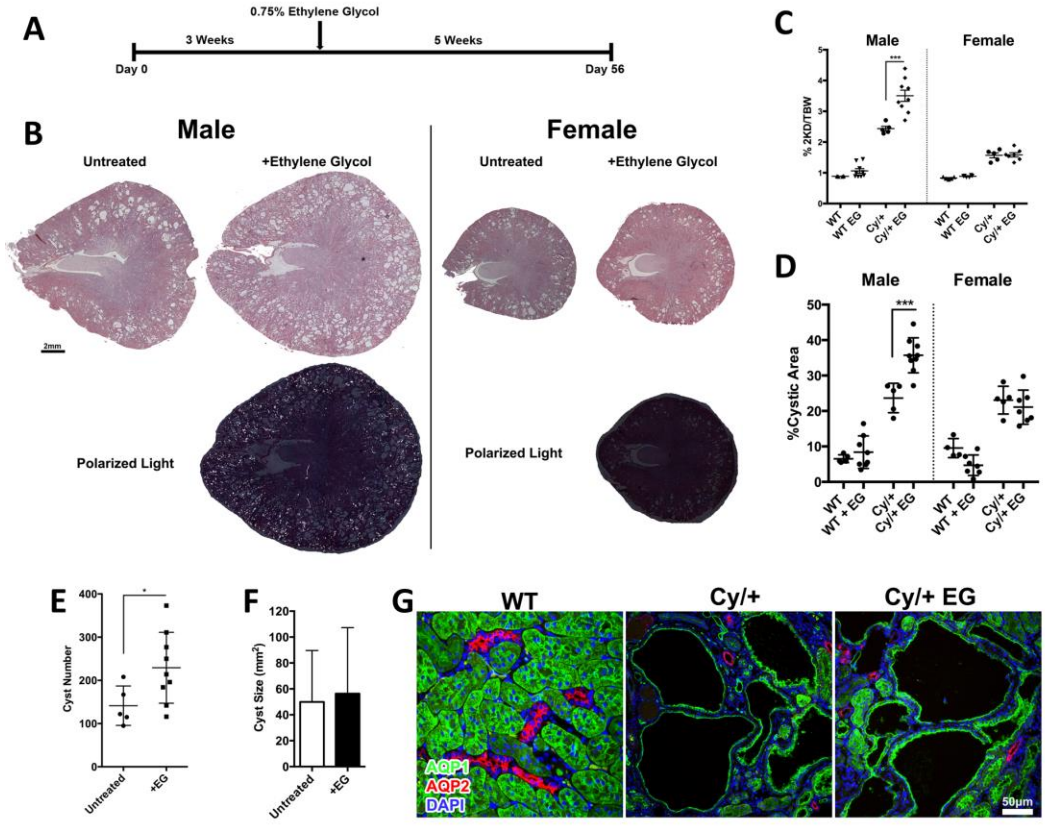

Figure 6: Ethylene Glycol treatment of Han rats exacerbates disease progression

A.) Rats were given 0.75% ethylene glycol in their drinking water starting at week 3 until 8 weeks of age. **B.)** Hematoxylin and Eosin stained kidney sections were visualized by light and polarized microscopy. **C.)** 2-Kidney/Bodyweight ratio from ethylene glycol treated and untreated rats. **D.)** Cystic Index of treated and untreated rats. ***>P=0.001. **E.)** Cysts counted from treated and untreated animals male Cy/+ rats. *>P=0.05 **F.)** Quantification of cyst sizes in ethylene glycol treated and untreated male Cy/+ rats. **G.)** Immunostaining with segment specific markers for proximal tubule (AQP1) in both ethylene glycol treated and untreated male Cy/+ rats. Error bars represent SD

Cysts are known to arise from the proximal tubule in Cy/+ rats[40]. Immuno-staining with segment-specific markers revealed that essentially all cysts are of proximal tubule origin in both ethylene glycol-treated and untreated male Cy/+ rats (Fig. 6G). This indicates that CaOx nephrolithiasis leads to increased cystogenesis only in the tubule segment that is predisposed to cyst formation in this model. Since female Cy/+ rats are exposed to the same ethylene glycol regimen as male Cy/+ rats but are resistant to renal CaOx crystal deposition and exhibit no altered cystic disease progression we conclude that the effect of ethylene glycol treatment in male Cy/+ rats is not due to any chemical action of ethylene glycol or oxalate *per se* but is due to the physical interaction of CaOx crystals with the renal epithelium.

Altogether, these results suggest that renal crystal burden can exacerbate cystogenesis leading to overall acceleration of PKD progression.

High phosphate diet leads to calcium phosphate crystal deposition and increased disease progression in the PCK rat model.

Next, we investigated whether the observed effect of renal crystal deposition on PKD progression is specific to CaOx crystals or may also be caused by crystals of a different chemical composition, and perhaps at a different location within the tubular/collecting duct system. We investigated the PCK rat model, an orthologous model to autosomal-recessive PKD that is due to a mutation in the *Pkhd1* gene[77]. In addition to liver cysts, PCK rats develop renal cysts of predominantly collecting duct origin which exhibit increased activity of mTOR[78,79], Src[80] and STAT3[30].

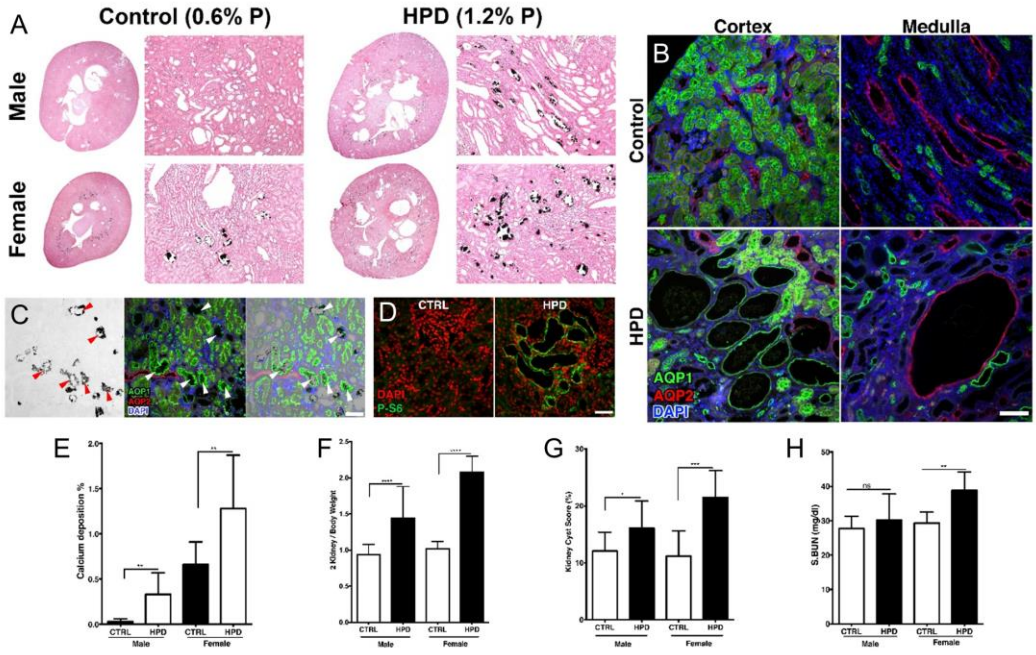

Figure 7: High phosphate diet induces calcium phosphate deposition and deterioration of disease progression in PCK rat model.
A.) Von Kossa staining in male and female PCK rats on control and high phosphate diet (HPD). **B.)** Quantification of CaP deposition in HPD male and female PCK rats**. C.)** 2-Kidney/Bodyweight ratio of control and HPD female and male rats. **D**.) Cystic index in HPD fed female and male rats **E.)** Blood urea nitrogen levels of control and HPD male and female rats. **F.)** Segment specific staining of HPD PCK rats shows appearance of new cortical cysts, which are originated from proximal tubules (AQP1 positive). **G.)** immunofluorescence staining of phospho-S6$^{S235/236}$ shows that the new cysts are highly positive for pS6. **H.)** Von Kossa and AQP1 and AQP2 costained sections indicate that crystals are located in the descending loop of Henle (AQP1 positive) not in the collecting ducts. Arrows denote crystals. Error bars represent SD. Scale bars are 100 μm (B), or 50 μm (C,D).

In contrast to CaOx nephrolithiasis that affects male humans and rats more severely than females, the opposite is true for CaP nephrolithiasis[60,81]. Dietary intake of phosphate varies widely among individuals and can influence the occurrence of CaP nephrolithiasis. To determine if increased dietary phosphate may affect PKD disease progression, male and female PCK rats were fed identical artificial diets except for the phosphorous content (control 0.6%; low phosphate

diet, LPD 0.2%; high phosphate diet, HPD 1.2%) between 3 and 10 weeks of age. LDP caused growth retardation compared to the control diet, but did not change cyst area or fibrosis (data not shown).

HPD led to a marked increase in CaP crystal deposits in tubule lumens along the corticomedullary junction, to a larger extent in female than in male animals (Fig. 7A, E). The location of CaP crystal deposition at the corticomedullary junction is consistent with previous findings[60]. Immunostaining for segment-specific markers revealed that CaP deposits occurred primarily in AQP1-positive tubules at the transition between proximal tubules and the thin descending loop of Henle (Fig. 7C). Strikingly, HPD led to a worse progression of PKD, to a larger extent in female than male animals. The two-kidney weight/body weight ratios (Fig. 7F) and cysts scores (Fig. 7G) were significantly increased in both male and female rats on HPD compared to controls (see also Suppl. Table 1). Female PCK rats in the HPD group also exhibited increased serum BUN values indicating impairment of renal function (Fig. 7H). In addition to an increase in AQP2-positive, collecting duct-derived cysts, HPD also led to the emergence of AQP1-positive and presumably proximal tubule-derived cysts (Fig. 7B). There was no effect on the liver cystic disease (Suppl. Table 1) suggesting that the effect of HPD is kidney specific. Altogether, these results show that a dietary-induced increase in tubular CaP precipitates leads to increased cystogenesis and PKD disease progression in this model. This location is consistent with the previous finding that CaP crystal deposition in female rats was generally localized to the corticomedullary junction[60], the location of the transition between proximal tubules and the loop of Henle.

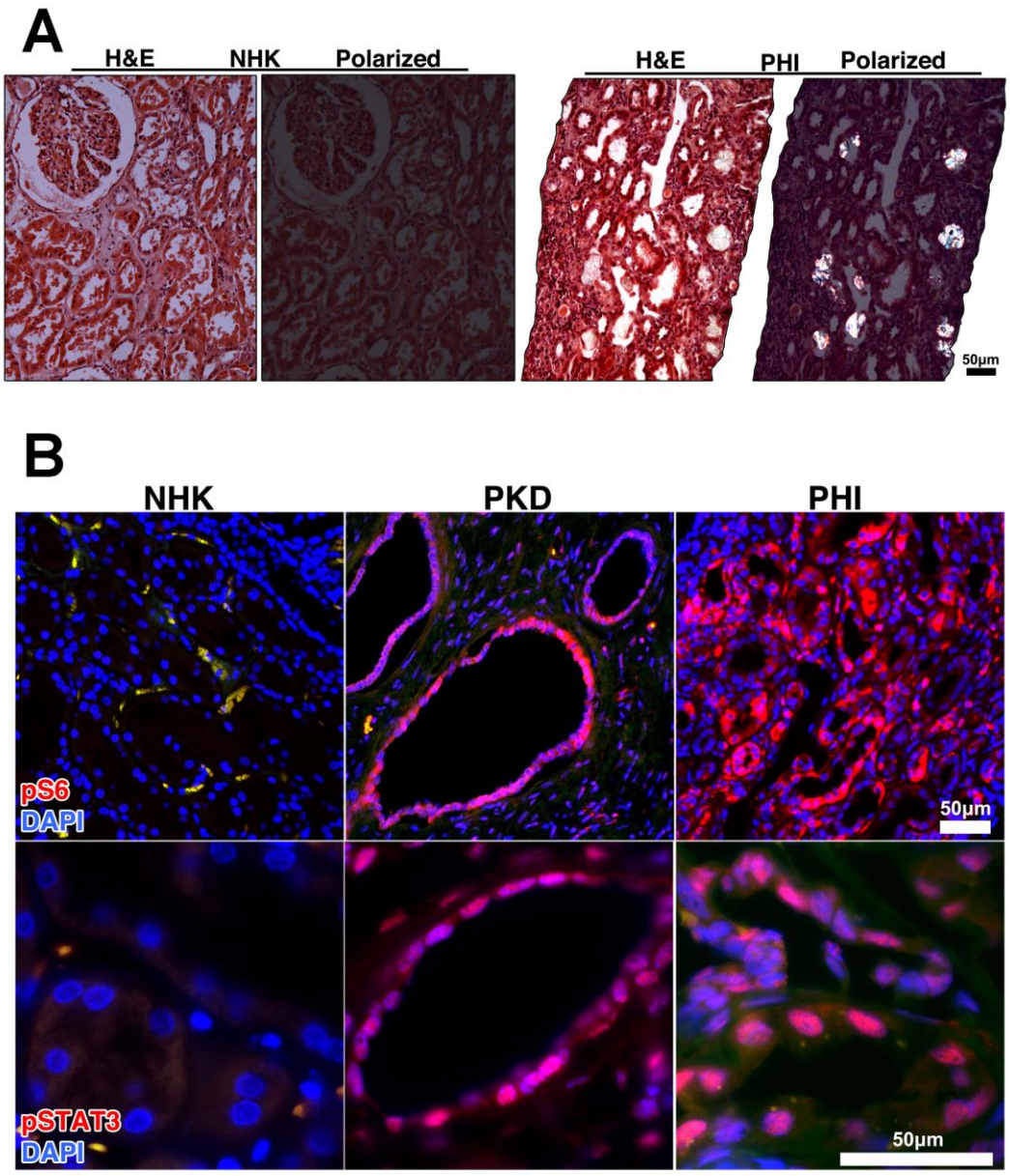

Figure 8: Human Primary Hyperoxaluric kidneys express PKD related signals

A.) Polarized images of Hematoxylin and Eosin stained kidney sections from a patient with primary hyperoxaluria type 1 (PH I) exhibit calcification of the kidney as evident by presence of birefringent crystal deposition, with tubular crystal deposition (n=3). **B.)** Immunostaining of PKD and PHI kidney sections for phospho-S6$^{S235/236}$ and phospho-STAT3^{Y705} shows strong signals for pS6 and pSTAT3 in the calcium deposited tubules (PH I) as well as dilated tubules and cysts in the human ADPKD samples.

HPD also caused a worse progression of polycystic kidney disease, again to a larger extent in female than male animals. The two-kidney weight/body weight ratios (Fig. 7C) and cysts scores (Fig. 6D) were significantly increased in both male and female rats on HPD compared to controls. Female PCK rats in the HPD group also exhibited increased serum BUN values indicating impairment of renal function (Fig. 7E). Segment specific marker immunostaining shows that the cysts are exclusively derived from the proximal tubules (Fig. 7F) and CaP crystals are deposited in the AQP1 positive cells (Fig. 7G) which stain the proximal tubules and thin descending loop of Henle. There was no effect on the liver cystic disease (not shown) suggesting that the effect of HPD is kidney specific.

Tubule dilation and activation of PKD-associated signaling pathways in human primary hyperoxaluria

To determine is these results can be validated our findings in human disease, we evaluated renal tissues from primary hyperoxaluria type 1 (PH1) patients. In PH1, a genetic defect leads to deficient glyoxylate metabolism, causing hyperoxaluria, CaOx nephrolithiasis and eventually renal failure. Renal biopsy specimens from PH1 patients exhibit CaOx crystal deposition and tubule dilation (Fig. 8A). Both mTOR and STAT3 pathways are strongly activated in PH1 to a degree comparable that seen in cysts in human ADPKD (Fig. 8B). This result suggests that tubular crystal deposition leads to activation of PKD-associated signaling pathways and tubule dilation in both rodents and humans.

Altogether, these findings are consistent with the conclusion that renal crystal deposition triggers accelerated progression of polycystic kidney disease by

activation of an inherent, renoprotective mechanism that has the purpose of facilitating the excretion of tubular crystals.

C. Discussion

The results presented here point to a previously unrecognized renoprotective mechanism that involves the purposeful dilation of renal tubules in response to lodged microcrystals with the apparent purpose of facilitating the "flushing out" of such crystals along the luminal space for excretion with the urine. Furthermore, our results suggest that this renoprotective mechanism acts as a "third-hit" trigger leading to accelerated disease progression in PKD.

Millions of microscopic crystals may form in human kidneys daily, are transported through the tubules, and excreted safely with the urine[49,82]. The presence of several types of crystals (incl. CaOx, CaP, struvite, uric acid) in urine is considered normal and up to a quarter of fresh urines from normal subjects even exhibit overt crystalluria[51] without immediate detriment to kidney function. Diets and numerous pathologies greatly influence the range of crystal burden that the kidneys experience. Without effective mechanisms to prevent excessive crystal growth and retention in tubular lumens, tubules would rapidly become occluded and renal function would seize. Protective mechanisms include renal regulators of crystal nucleation and growth such as osteopontin, nephrocalcin and THP[50]. However, the occurrence of nephrocalcinosis and nephrolithiasis indicates that these mechanisms are not always completely effective, and that crystals can sporadically lodge in tubule lumens due to aberrantly fast growth or aggregation. It is poorly understood how sporadically lodged micro-crystals are cleared from kidneys. One observed mechanism is that some crystals can somehow cross the

epithelial barrier into the interstitial space presumably via endocytosis[52]. However, their subsequent fate is uncertain and this may be a slow process occurring in the time-frame of weeks[83]. It is difficult to see how such a cumbersome and disruptive interstitial mechanism could accomplish effective clearance of more than a small amount of lodged crystals at a time. What is known, is that, eventually, renal crystal deposition can lead to pathological nephrocalcinosis or nephrolithiasis including tubule occlusion and the formation of macroscopic kidney stones which are most commonly found in the urinary space attached to the renal papilla[83–86]. Roughly 70-80% of all kidney stones in humans are composed of CaOx.

Even though tubule dilation is universally observed in many forms of nephrocalcinosis and nephrolithiasis in humans and animal models[87] this phenomenon has not been considered of anything more than a secondary consequence to cell injury. Our results suggest that CaOx crystal deposition leads to very rapid activation of mTOR and Src/STAT3 signaling in tubule epithelial cells accompanied by equally rapid dilation of tubule diameters. While occasional cell damage can be observed – particularly when cells are in direct contact with a lodged crystal - the rapid dilation response occurs in most tubule segments up- or downstream of any lodged crystals without any apparent evidence of cell damage or death. Our results suggest that segments all along an affected nephron will dilate in response to lodged CaOx crystals, whether a crystal is detectable in the particular segment under observation or not.

We have chosen experimental conditions of oxalate challenge that lead to a moderate degree of initial deposition of CaOx crystals, which can eventually be completely resolved by the kidneys. This level of crystal burden does not lead to

widespread tissue destruction or renal failure, and was meant to mimic the situation that kidneys may frequently be exposed to under non-pathological conditions. We find that CaOx crystals under these conditions are located almost exclusively in tubule lumens from the moment they first occur until they are cleared. Interstitial crystals are very rarely observed. This suggests that the vast majority of crystals are cleared via the luminal space and excreted with the urine. The distribution of acutely induced CaOx crystals indicates that crystals initially form in the proximal tubule and are then passed all along the tubular system. This is in agreement with previous studies in rats[87] and primary hyperoxaluria patients[88]. It is intuitive that dilation along the entire length of the nephron would facilitate this mechanism of "flushing out" crystals and counter their accumulation. Indeed, we find that mTOR inhibition with rapamycin blunts the ability of tubules to dilate in response to CaOx crystals and leads to accumulation of crystal aggregates, primarily at the transition from the proximal tubule to the descending loop of Henle. These transitions are located in the corticomedullary boundary and appear to represent a bottleneck for the passage of microcrystals, presumably due to the abrupt narrowing of tubule diameters. This is consistent with the previous finding of CaOx crystal aggregates in the same location in primary hyperoxaluria patients[88].

We propose that tubule dilation is a purposeful mechanism that involves activation of mTOR and STAT3 signaling pathways. Several possible scenarios can be envisioned for how a CaOx crystal may trigger a dilation response in tubule epithelial cells. In a possible short-range mechanism, the direct physical contact of a crystal with the apical surface of epithelial cells may be required while the

crystal passes through a tubule. This model, however, would not explain how a tubule segment downstream of a lodged crystal would be able to detect its presence and dilate in response. Alternatively, in a possible long-range mechanism, a lodged crystal may activate a response both up- and downstream of its location by affecting the fluid flow in the given nephron due to partial or complete occlusion. Other possible long-range mechanisms may involve diffusible factors – such as growth factors, cytokines or other signaling molecules – that may be secreted by injured epithelial cells in direct contact with a crystal or mechanical stretching sensed by the tubular cells. Primary cilia may potentially play a role in both short- and long-range mechanisms by sensing of crystals, signaling factors and/or fluid flow. Future work is required to investigate these possibilities.

Our results suggest that tubule dilation involves - and at least partially requires - activation of mTOR signaling. mTOR functions in two complexes, mTORC1 and mTORC2, which regulate numerous cellular functions including cell size, proliferation and the actin cytoskeleton[89,90]. It is possible that an mTOR-dependent cell size increase may play a role in tubule dilation. Our finding that dilation of tubule diameters comes at the expense of cell height indicates that a change in cell shape is important raising the possibility that mTOR-mediated changes in the actin cytoskeleton may play a role in this process. Interestingly, *Pkd1*$^{-/-}$ cyst-lining epithelial cells also exhibit a change in shape from cuboidal to flat[91] which suggests that polycystin-1 may have a role in cell shape regulation. It is important to note that PC1 can regulate mTOR activity[8,92] suggesting a coupled pathway. It was also recently shown that osteoblastic cells react to stretch by PC1-dependent activation of STAT3[93]. Whether PC1 plays a direct role in the

regulation of mTOR and/or STAT3 signaling during the dilation-response to crystal deposition shown here remains to be investigated.

In addition to a relatively rapid response of dilation of tubule diameters, peaking at 24 hours, we also observe a slower induction of proliferation, peaking at 3 days after acute oxalate challenge. The later proliferative phase may aid in the replacement of damaged cells. Consistent with this view, it has been found that CaOx crystals can lead to necroptosis of tubule epithelial cells[94]. mTOR activation appears to be involved in the proliferative response because rapamycin treatment strongly inhibits proliferation of tubule cells in response to CaOx crystal deposition (Fig. 4C). Our results, however, suggest that mTOR and STAT3 activation are independent of each other because STAT3 is still activated in the presence of rapamycin (Fig. A, B).

In the natural progression of PKD, tubule dilation is the first step towards cystogenesis. Recent evidence from several laboratories clearly indicates that genetic inactivation of *Pkd1*, or ablation of primary cilia in mice with mature kidneys, is insufficient to trigger cystogenesis. However, subsequent renal insults can trigger rapid cystogenesis in such models, which has led to the now widely accepted view that a "third-hit" mechanism determines the rate of cystogenesis and progression in PKD. Experimentally, ischemia-reperfusion injury, nephrotoxic injury and compensatory hypertrophy after uninephrecotomy have been shown to act as third-hit triggers in preconditioned mice. Given that such types of renal insults are rare in humans, they appear unlikely to explain the relatively steady rate of progression in human ADPKD. Our results suggest that activation of the

renoprotective mechanism in response to crystal deposition described here can act as a third-hit trigger and accelerate the rate of PKD progression.

We found that tubule dilation in response to crystal deposition involves activation of the same signaling pathways, mTOR and Src/STAT3, that have previously been shown to be involved in PKD. In this process, mTOR-dependent proliferation is also activated, as it is in PKD. In two rat models of PKD we showed that conditions that lead to renal deposition of different types of crystals also lead to increased cystogenesis and accelerated disease progression. These rat models are genetically independent of each other and exhibit different disease phenotypes. The gene coding for Samcystin, a protein expressed in proximal tubule cells[95], is affected in the Han:SPRD rat model which leads to cysts of proximal tubule origin[16]. In contrast, the gene coding for fibrocystin is affected in the PCK rat model[77] which leads to cysts of collecting duct origin. The functions of Samcystin and fibrocystin are incompletely understood. Samcystin interacts with Bicc1[96] which, is an RNA binding protein that localizes and silences bound mRNA[97] and acts both downstream and upstream of the polycystins[98,99], the proteins affected in human ADPKD. Fibrocystin, which is mutated in human ARPKD, co-localizes with the polycystins on primary cilia, physically interacts with polycystin-2[36], and has been shown to regulate mTOR activity[100] similar to polycystin-1[8]. It is likely that most or all the ciliopathy-associated proteins converge on the same molecular pathways that lead to renal cyst growth. In human ADPKD, cysts arise from all nephron segments, and therefore the PCK and Han:SPRD models may be regarded as models for subsets of cysts that arise from distinct tubule segments. Nevertheless, despite this genetic and phenotypic

distinctness between these two models, and even though we induced deposition of crystals of different chemical compositions (CaP vs. CaOx) we observed an increase in cystogenesis in both cases. These results suggest that renal crystal deposition can lead to cystogenesis in a variety of tubule segments and in a variety of genetically predisposed models.

Our results indicate that the observed increase in cystogenesis was dependent on the physical presence of tubular crystals as opposed to any effects of oxalate or phosphate per se. Treatment of male and female Han:SPRD rats with the same dose of ethylene glycol resulted only in crystal deposition and increased cystogenesis in males but not females. Similarly, the effect of a high phosphate diet on CaP precipitation correlated with increased cyst growth preferentially in female rather than male PCK rats. This suggests that increased cystogenesis is due to mechanical effects of crystals, such as possibly disruption of fluid flow or physical cell damage.

Based on these results, we propose that renal crystal deposition may affect disease progression in human ADPKD. Although there is no definitive study, a link between ADPKD progression and renal crystal burden has emerged based on numerous correlative studies. Generally, in these studies it is speculated that increased abnormalities in tissue architecture and/or metabolic abnormalities during ADPKD progression may be the cause of increased nephrolithiasis. However, the opposite may be the case; i.e. that increased crystal burden leads to accelerated ADPKD progression. It is also possible that ADPKD progression and nephrolithiasis positively reinforce each other leading to a vicious cycle.

If nephrolithiasis accelerates ADPKD, then treatments that reduce renal crystal formation and deposition may slow progression in ADPKD. Such treatments typically are dietary changes to avoid foods rich in oxalate, phosphate, and uric acid precursors, increased water intake, and supplementation with citrate as a chelator of calcium to reduce CaOx and CaP precipitation.

Remarkably, increased water intake has already been shown to effectively slow PKD progression in the PCK rat[27]. The mechanism of the protective effect is unknown, but was hypothesized to involve a decrease in vasopressin signaling. We hypothesize that the protective effect may instead (or in addition to) be due to increased urine output and dilution of solutes, which decreases the risk of tubular crystal deposition. Increased water intake is commonly prescribed for the treatment of recurring nephrolithiasis in humans.

Even more remarkable, citrate treatment has been shown to be highly effective in reducing cyst growth, preserving renal function and extending life span in the Han:SPRD rat model[64–66]. The mechanism of this effect remained unexplained and these investigators speculated that the effect may be due to alkalization of the urinary pH. In contrast, we hypothesize that the beneficial effect of citrate observed in those early studies was due to citrate's action as a chelator and inhibitor of calcium crystal formation. For this reason, citrate is a standard treatment for patients with recurring calcium nephrolithiasis[101]. Unfortunately, presumably due to the lack of a mechanistic explanation, citrate has never been tested in clinical trials in ADPKD patients. Citrate was found to be ineffective in the pcy mouse model of PKD[102,103]. However, this was likely due to the fact that tubular crystals play no role in the cystogenesis of this, or any other, mouse model

because mice are naturally highly resistant to CaOx crystal precipitation. Furthermore, cystogenesis in most genetic mouse models of PKD is pre-determined by the genetic abnormality and does not depend on any third hit trigger. Consistent with this, no evidence for lithogenic risk factors were found in a Pkd1 mouse model[104].

D. Methods

Animals

All animal experiments were conducted under the supervision and approval of the UCSB Institutional Animal Care and Use Committee (IACUC). Animals maintained and produced at UCSB were housed in the animal resource center with a 12-hour light/dark cycle, allowed free access to water and standard chow with wood based bedding. When available, breeders were provided with housing enrichment in the form of cardboard tubes (rats) or plastic housing (mice). All animals were weaned at 3 weeks of age and separated by sex. Genotype of animals was not used to sort animals into cages prior to treatment. All animals were monitored for signs of distress during the course of the study including: poor grooming, changes in mobility, abnormal posture, abnormal gait and unkempt appearance. Individual animals were treated as the experimental unit for the purposes of this study. The researchers performing the experiments were not blinded to the treatment of animals.

Sample Size

Sample size was determined using prior knowledge from experiments performed in our lab using polycystic animals[69,105].

NPT2a Deficient Mice

4-6 month-old *Npt2a*-KO mice weighing 18-30g were given 1.5% glyoxylate or 1.25% ethylene glycol mixed with chow for 28 days to induce hyperoxaluria after which mice were sacrificed. By day 7 of the experiment *Npt2a* -/- mice became hyperoxaluric, and remained so throughout the experimental period.

Oxalate Treatment

All injections of oxalate were performed between 8-10AM in the animal resource center via intraperitoneal administration to control the dose of oxalate.

Mice

8-10 week-old male and female C57/B6 mice weighing between 20-30g were purchased from Charles Rivers laboratories and allowed 1 week to acclimate to our animal facilities. Mice were challenged with a single intraperitoneal injection of 0.22M sodium oxalate dissolved in 0.9% saline, sterile filtered and administered at 3mg/100g (low dose) and harvested at 6 hours (n=4), 1 day (n=12), 3 day (n=8) and 7 days (n=10); or 7mg/100g (high dose) at 3 hours (n=4) and 1 day (n=9) to produce oxalate crystals. Control animals included n=6 males and n=5 females treated with saline. Low dose animal trials were conducted in 5 separate experiments and high dose trials were conducted in 2 separate experiments. Animals that did not exhibit crystal deposition were not included in analyses of crystal effects.

Sprague Dawley Rats

8-week-old Sprague Dawley rats weighing between 200-300g were purchased from Charles Rivers laboratories and allowed 1 week to acclimate to our animal facilities. Prior to treatment, animals were grouped into 2-3 per cage and treated

identically. Rats were challenged with a single intraperitoneal injection of 0.22M sodium oxalate dissolved in 0.9% saline, sterile filtered and administered at 7mg/100g and harvested 6 hours (n=5), 1 day (n=5), 3 days (n=5), or 7 days (n=3) to produce oxalate crystals. 6 hour, 1 day and 3 day treatments were conducted over 3 experiments and once for 7 days. ***Rapamycin treatment-*** Prior to oxalate challenge, Sprague Dawley rats were treated with 2mg/kg rapamycin (LC Laboratories) dissolved in DMSO 18 hours prior to oxalate administration, then 24 hours after oxalate administration and finally 72 hours following oxalate administration. Controls received DMSO only. Rapamycin treated animals were treated with oxalate as described above and harvested 6 hours (n=5), 1 day (n=5), 3 days (n=5), or 7 days (n=2). 6 hour, 1 day and 3 day treatments were conducted over 3 experiments and once for 7 days. 5 age-matched untreated controls were used for this experiment. Animals that did not exhibit crystal deposition were not included in analyses of crystal effects.

Han:SPRD Rats

The Han:SPRD rats were graciously contributed by Benjamin Cowley and transferred to the animal resource center at the University California Santa Barbara.

Genotyping

Rats were genotyped using a known polymorphism in the *Ansk6* (*Pkdr1*) gene. PCR coupled to restriction digest was used detect a C to T transition responsible for PKD in the Han:SPRD rats. Normal and Cy/+ rats were genotyped using a PCR restriction fragment length polymorphism method as described previously by Brown et al.[16]. DNA was extracted from a small piece of ear of each rat and PCR

products were obtained from each DNA sample. Primers for rat Samcystin were as follows: sense primer: CTA GAA GCC TCA GTG ACC CC; anti-sense primer: CAG CGT GTG AAC AAG GTA GG. Amplification products were digested by Msp1 (Fermentas) at 37°C for 1 h. Digested PCR products were resolved on an agarose gel, producing bands at 157 and 85 bp; 242, 157, and 85 bp; and 242 bp for +/+, Cy/+, and Cy/Cy rats, respectively.

Ethylene Glycol Administration

Ethylene glycol (Sigma-Aldrich) was prepared at 0.75% in purified water and administered ad libidum from 3 to 8 weeks of age. Animals treated for this experiment include; 9 wild-type male rats (264.0g±22.9), 9 Cy/+ male rats (251.1g±21.6), 6 wild-type female rats (202.8g±17.4), 7 Cy/+ female rats (188.9g±14.3). Untreated animals include; 4 wild-type male rats (274.3g±16), 5 Cy/+ male rats (267.3g±16.6) and 5 wild-type female rats (192g±12.1), 5 Cy/+ female rats (193.8g±13.4).

PCK Rats

Male and female PCK rats were fed identical diets except for phosphorous content. 10 male rats (387.2g±20.0) and 10 female rats (245.3g±12.8) were given 0.6% (Intermediate phosphorous) or 10 male rats (344.7g±12.0) and 10 female rats (227.6g±8.4) were given 1.2% (High phosphorous) diets from 3 to 10 weeks of age.

Hematoxylin and Eosin Staining

Paraffin embedded tissues were cut into 5µM sections using a microtome and placed onto Superfrost+ slides (Fischer Scientific). These sections were then dried overnight on a hot plate at 37°C before moving through a rehydration series

(xylene, 100%EtOh, 95%EtOH, 70%EtOH). Slides were then rinsed in distilled water briefly, immersed in hematoxylin for 45secs and rinsed with tap water until no more hematoxylin residue was observed. The slides were then dipped 10 times in 95% EtOH before placed in Eosin Y solution for 45secs. The slides were then dipped 10 times in 95% EtOH, 10 times in 100% EtOH twice and xylene for 5 minutes twice. After which the slides were sealed using Permount mounting media (Fischer) and covered with a coverslip.

Von Kossa Staining

Following rehydration in ethanol, samples were incubated in 5% silver nitrate solution for 30 minutes exposed to UV light. Samples were then rinsed in distilled water and incubated in 5% thiosulfate solution for 3 minutes followed by a 2-minute rinse in running tap water and 2 rinses in distilled water.

Immunofluorescence

Formalin fixed, paraffin embedded kidneys were sectioned to 5µm thickness using a microtome. Samples were then rehydrated as described for H and E staining. Following rehydration slides were washed in TBS and boiled in trisodium citrate at pH 6 for 5 minutes in a pressure cooker. Once cooled the slides were washed twice by TBST (each 5 minutes) and blocked by blocking buffer (1% BSA, 0.1% Fish skin gelatin, 0.05% Sodium Azide in TBST) at 37˚C for 30 minutes. After which the blocking buffer was aspirated and the slides were incubated with primary antibody diluted 1:200 in blocking buffer overnight at 4˚C (Rabbit anti-pS6$^{S235/236}$, Cell Signaling #4858; Rabbit anti-pSTAT3^{Y705}, Cell Signaling #9145; Rabbit anti-aquaporin-1, Millipore AB2219; Goat anti-aquaporin-2, Santa Cruz sc-9880; Mouse anti-Calbindin D-28K, Sigma C9848; Rabbit anti-Tamm-Horsfall

protein, Santa Cruz sc020631; Rabbit-anti-Ki-67, BD Pharmingen #550609). The following day, to quench background auto-fluorescence, the slides were incubated with 1% Sudan Black diluted in 70% ethanol for 20mins which, followed by two washes in TBST each for 5 minutes while gently agitated. The slides were then incubated with a species-specific fluorescently conjugated 2˚ antibody diluted in blocking buffer at 37˚C for one hour (Goat anti-Rabbit-DyLight 488 and 594, #35552 and #35560, ThermoFischer; Goat anti-mouse-DyLight 488, ThermoFischer #35502; anti-LTL-FITC, Vector FL-1321; anti-DBA-Rhodamine, Vector RL-1032). The slides were next washed in TBST 3 times for 5 minutes with agitation followed by fixation using 4% paraformaldehyde for 5 minutes and finally washed in TBST. Slides were then covered with ProLong w/DAPI (ThermoFischer) and covered with a coverslip.

Cystic Index

Whole kidney sections stained with Hematoxylin and Eosin were used to determine cystic indices. Sections were analyzed using ImageJ software to determine the amount of white space relative to total kidney area. Manual determination of inclusive areas was used to exclude artifacts from section preparation (i.e. holes, debris, etc.). Each sample was measured three times with the average used for analysis.

Crystal Aggregate Analysis

Crystal aggregates were counted and scored using ImageJ software. 7-10 fields from 20x images were obtained from both cortical and medulla areas of kidney sections from treated animals before being analyzed. Aggregates were determined to be clusters of crystals within a single tubule.

Polarizing Microscopy

Polarizing microscopy was used with H & E prepared tissue sections to observe the presence of birefringent oxalate crystals.

Cell Height, Tubule and Lumen Diameter

Tubule diameter was measured from the basal membrane across the narrowest segment of the tubule to the basal membrane of the opposite side of the tubule. *Lumen diameter* was determined by measuring the brush border to the brush border of the narrowest portion of the tubule. *Cell height* was determined by measuring three cells per dilated tubule, measuring the cell height from the basal to apical membrane across a cell nucleus. The researcher performing the measurements was blinded to the treatments.

Western Blotting

Sample Preparation-Tissues were removed from animals, bisected sagittally, and placed into a mortar cooled with liquid nitrogen, submersed in liquid nitrogen and pulverized using a pestle. These samples were then placed into microcentrifuge tubes and stored at -80˚C for future analysis. Approximately 10mg of tissue were lysed in 200µL of 4% SDS-100mM Tris pH 6.8 lysis buffer containing phosphatase and protease inhibitors (Phosphatase inhibitor cocktail 2 & 3 (Sigma-Aldrich), PMSF, Protease Inhibitor cocktail (Sigma-Aldrich)). These samples were then extensively vortexed and heated at 100˚C for 10 minutes followed by extensive vortexing. The samples were then centrifugated at 13g for 10 minutes to pellet non-soluble cell debris. The supernatant was then transferred to a new microcentrifuge tube and protein concentrations were determined using a NanoDrop spectrometer reading absorbance at 280nm.

***SDS-PAGE and Antibodies*-**Bromophenol blue and 50mM DTT were added to protein samples in 2% SDS-50mM Tris pH 6.8 buffer prior to being heated at 100˚C for 5mins to reduce disulfide bonds. Samples were then loaded at standard concentrations of 50µg per well using 10% acrylamide gels for SDS-PAGE. The gels were run for approximately 90mins at 100V followed by transfer onto nitrocellulose membranes at 100V for 90mins in an ice bath. The membranes were blocked using 5% BSA-TBST for 20mins at 37˚C followed by 3, 5min rinses in TBST. The membranes were then incubated overnight at 4˚C on a rotator in primary antibody solutions containing 5% BSA-TBST (Mouse anti-Actin, Amershan Bioscience N350; Rabbit anti-pS6$^{S235/236}$, Cell Signaling #4858; Rabbit anti-total-S6 Cell Signaling #2217; Rabbit anti-Src, Cell Signaling #2109; Rabbit anti-pSrc^{Y416} #6943; Rabbit anti-pSTAT3^{Y705}, Cell Signaling #9145; Mouse anti-STAT3, Cell Signaling #9139). The following day the membranes were washed 3 times for 5 minutes in TBST and incubated in the appropriate species specific fluorescent or HRP conjugated secondary antibodies (Goat anti-mouse-IR Dye 800CW, Li-Cor #926-32210; Donkey anti-rabbit-IR Dye 680, Li-Cor #926-32221, Goat anti-rabbit HRP, Jackson ImmunoResearch #111-035-144, Goat anti-mouse HRP, Jackson ImmunoResearch #115-035-044) in 5% Dry Milk-TBST for 45mins at 25˚C under agitation while preventing exposure to external light sources. The membranes were then rinsed in TBST for 15mins before visualization using chemiluminescence (Pierce) or LiCor scanner.

TUNEL Assay

Apoptosis was measured by TUNEL assay (Click-iT® Plus, cat. No. C10617, Thermo Fisher Scientific). Apoptotic nuclei and DAPI positive cells per field were counted.

Statistical Analysis

Data sets were tested for normality prior to a nonparametric, one tailed, Mann-Whitney analysis with Prism graphing software. All graphs display the standard deviation. Box whisker plots represent 90% of values with median displayed as a line in between the 2nd and 3rd quartiles and the mean displayed with "+". Variances between statistically compared groups differed.

Human PH Samples

Human primary hyperoxaluric samples (n=3) were donated from Dr. Bernd Hoppe from Universitätsklinikumbonn Germany.

Data Availability

Data requests are available from the corresponding author.

Author Contributions

Jacob Torres contributed animal procedures, immunofluorescence, western blotting, histology and statistical analysis. Mina Rezaei contributed immunofluorescence, Von Kossa staining, statistical analysis, and histology. Louis Lin contributed immunofluorescence data. Caroline Broderick contributed western blotting and tubule measurements. Benjamin Cowley contributed Han rats for experiments. Vicente Torres contributed PCK rat experiments. Saeed Khan contributed all NPT2a -/- animals for analysis. All experiments were conducted under the supervision of Thomas Weimbs.

III.

The Soluble C-terminal Tail of Polycystin-1 Interacts with mTOR, Mitochondrial Associated Proteins, and Protects Against Calcium Induced Cytotoxicity

Abstract

Polycystin-1 (PC1) is the primary protein associated with the initiation of ADPKD, accounting for 85% of the cases reported. PC1 is a large multi-pass integral membrane protein that contains a 200-amino acid C-terminal cytoplasmic tail. Under certain cellular conditions, the cytoplasmic tail of PC1 may undergo proteolytic cleavage to produce a soluble 30kDa fragment (p30). The p30 fragment may then undergo translocation to the nucleus and coactivate STAT3 mediated gene transcription[30]. It has been observed that the cyst lining epithelia cells in ADPKD kidneys exhibit increased levels of the cytoplasmic PC1 tail within the nucleus[106] and increased levels of active STAT3 (Fig. 8). We therefore hypothesized that the small p30 fragment may be a critical regulator in the initiation and maintenance of ADPKD. Here I show that p30 interacts with the primary target of rapamycin, mTOR, a critical regulator of cell growth, and proliferation in ADPKD and additionally associates with the mitochondrial proteins AIF and the ATP synthase β-subunit. Drug treatment with the ionophore, ionomycin and p30 expressed in MDCK cells showed resistance to calcium induced cytotoxicity. Taken together, these data show p30 involvement in mTOR signaling, oxidative phosphorylation, programmed cell death and the protective effects observed from ionomycin induced calcium cytotoxicity.

A. Introduction

The cytoplasmic tail of polycystin-1 contains a 200 amino acid intracellular domain that can be cleaved by γ-secretase[107] at the membrane to form a soluble 30kDa fragment (p30/FLS). This terminal p30 fragment appears to be an important region for protein interactions and signaling. The structure of the tail is predicted to be a coiled-coil domain containing a cleavage site for Caspase-1[22], a PEST domain, a calmodulin binding domain[108] and has been shown to bind to multiple proteins that are involved with DNA repair, energy metabolism and apoptosis (Fig. 10). Following cleavage by Caspase-1, the p30 fragment is split into a smaller active fragment, p15, that also appears to have biological activity[22].

The increase in STAT3 activity is believed to be part of the mechanism for cyst formation and may be exacerbated by aberrant coactivation of p30. Following injury, PC1 is cleaved at the membrane to release the soluble p30 fragment whereby it translocates to the nucleus and coactivates STAT3 gene transcription. The cleavage and translocation of p30 has been observed in unilateral ureteral obstructed mouse kindeys[106]. This translocation into the nucleus can be mediated by expression of PC2 and the activity of p30 appears to require its nuclear localization to mediate gene transcription[106].

The small soluble p30 fragment has been shown by our lab to coactivate STAT3 gene transcription via a dual mechanism[6]. This dual activity of p30 occurs from its ability to increase STAT3 gene transcription via the activation of Src or Janus kinase (JAK) activity (Fig. 9). The IL-6 receptor mediates the activation of JAK signaling whereas increases in c-AMP or extracellular growth factors activate Src. Paradoxically, upregulation of suppressor of cytokine signaling 3 (SOCS3)

and STAT3 activation are both observed in human ADPKD cyst lining epithelia cells[30]. Increased levels of cytokines and growth factors are also observed within cyst fluid[31] which may be the cause of activation. In ADPKD, the activation of STAT3 is accompanied by an increase in SOCS3, implying that the activation of STAT3 is occurring from an alternative pathway mediated by Src.

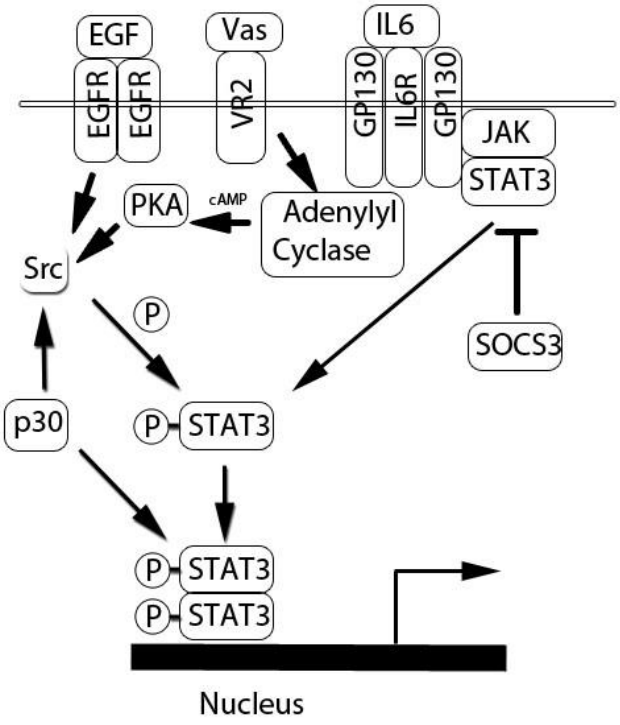

Figure 9: **Proposed signaling mechanism involving the p30 fragment of polycystin-1:** p30 can coactivate STAT3 gene transcription through its ability to directly increase STAT3 activity, or by increasing the activity of Src which in turn phosphorylates STAT3. STAT3 can be phosphorylated via the IL6/JAK pathways or through the activation of Src through increases in cAMP and PKA, or EGFR phosphorylation.

STAT3 phosphorylation can occur from the IL-6 Receptor/GP130 activation JAK, and alternatively by EGF receptor or vasopressin receptor activation of Src. The activation of the EGF receptor directly activates Src through its tyrosine kinase activity and activation via vasopressin leads to an increase in intracellular cyclic AMP and Src activity through protein kinase A (Fig. 9).

Research on the vasopressin receptor antagonist Tolvaptan has shown moderate success in ameliorating PKD in human patients, but with side effects that make compliance challenging. Reduction of cysts in response to vasopressin antagonism and high levels of cAMP in cyst fluid implicates the activation of Src via PKA.

In addition to the regulation of STAT3, the C-terminal tail of PC1 has been shown to be directly involved in the negative regulation of mTOR signaling by its interaction with the Tuberous Sclerosis protein Tuberin (TSC2)[29]. When the PC1 tail is tethered to the membrane it is capable of repressing mTOR activation by keeping TSC2 sequestered at the membrane. This fits with the observation of increased mTOR activity in ADPKD cyst lining cells and the increase in PC1 C-terminal cleavage following injury[106].

The activation of p30 in response to injury in is believed to be a normal response for the cell in initiation of the repair response. In ADPKD, cystic cells are unable to cease the cycle of PC1 cleavage, mitogenic signaling, and p30 coactivation of STAT3. This cycle of activation by p30 we believe is involved in a futile repair response, resulting an excessive proliferation following injury.

The dysregulation of mTOR signaling appears to underlie the pathology of ADPKD. I investigated if there is a direct physical interaction between the C-terminal tail of polycystin-1 and mTOR. The Tuberous Sclerosis complex (TSC) comprised of Hamartin/Tuberin (TSC1/TSC2) proteins negatively regulates mTOR. The function of TSC2 is to activate the G-protein Rheb that in turn activates mTOR complex 1 (mTORC1). When TSC2 is bound to the membrane tethered TSC1, the TSC is formed and TSC2 is sequestered on the plasma membrane in its inactive form and the activity of mTORC1 is inhibited.

B. Results

p30 and mTOR

To test if there is an interaction between the C-terminal tail of PC1 and mTOR, tagged versions of both p30 and mTOR were used. HEK293t cells were transfected with membrane bound p30 ("Full Length Soluble Membrane Bound" or FLM) and the soluble tail of PC1 ("Full Length Soluble Fragment" or FLS/p30), followed by affinity chromatography and immunoblotting (Fig. 10).

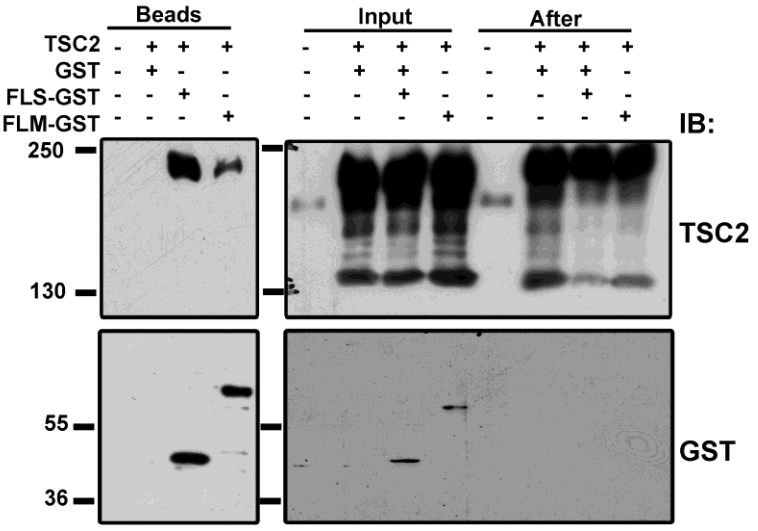

Figure 10: Interaction between the C-terminus of PC1 and TSC2: HEK293t cells cotransfected with TSC2 and GST tagged FLS/p30 (FLS-GST) or GST tagged membrane bound FLS/p30 (FLM-GST). Both GST-FLM and GST-FLS bound to TSC2 with the soluble form of FLS showing a higher affinity. "Input" samples are whole cell lysates used for the experiment. "After" samples represent depleted samples following GST pull down.

When TSC2 was cotransfected with the soluble tail of PC1 (FLS-GST), there was an increase in the amount of protein bound to the beads relative to the membrane tethered version of the PC1 tail (FLM-GST). This direct interaction between the C-terminus of PC1 and TSC2 has also been investigated by Dere et al and shown to inhibit mTORC1 signaling[29]. After verifying that there was an

interaction between p30 and the mTOR regulator TSC2, I next investigated the possibility that mTOR interacts with p30. HEK293t cells were transfected with mTOR and either soluble or membrane bound p30 (Fig. 11).

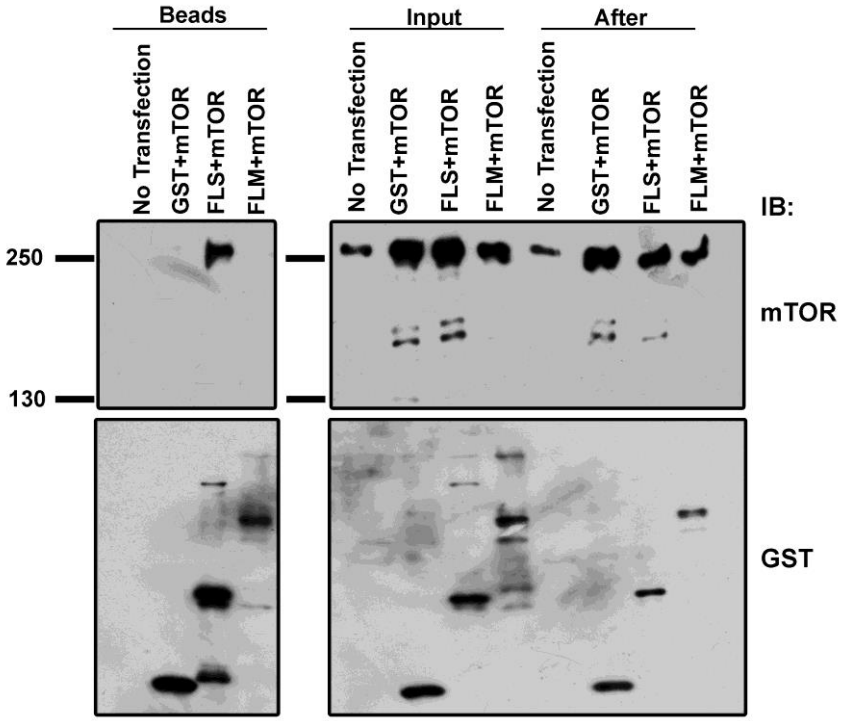

Figure 11: Interaction between of a soluble or membrane bound form of the PC1 c-terminal tail in CHAPS buffer: HEK293t cells cotransfected with mTOR and GST tagged FLS/p30 (FLS-GST) or GST tagged membrane bound FLS/p30 (FLM-GST). mTOR bound with the soluble form of FLS and not membrane bound. "Input" samples are whole cell lysates used for the experiment. "After" samples represent depleted samples following coimmunoprecipitation.

A strong interaction with mTOR was observed with the soluble fragment but no interaction was observed with the membrane bound p30. Attempts to isolate the mTOR/p30 interaction using standard coimmunoprecipitation buffers containing Triton detergent were unsuccessful. Using CHAPS buffer allowed for detection of mTOR with p30, presumably this is because mTOR's interaction with p30 is through another protein interaction complexed with mTOR that is disrupted

by more harsh detergents. I next tested where the binding of mTOR to p30 may be occurring. Cotransfection of mTOR with two C-terminal deletion constructs of p30 (amino acids 4107-4272 (165AAs) and 4107- 4195 (88AAs) of PC1) showed that the binding of mTOR to p30 is inhibited nearly equally following the truncation of the last 41 residues of the C-terminus (Fig. 12).

These data show that PC1 may be directly involved in the regulation of mTOR through binding of the PC1 C-terminus to both TSC2 and mTOR, either as part of a complex or direct interaction. Because this is an overexpression model, more investigation into the function of this interaction will be necessary to determine if this interaction does in fact regulate mTOR signaling.

This experiment places mitochondria front and center in PKD as more evidence mounts to implicate glucose necessity and defective cellular metabolism as a hallmark of PKD.

As a first step in investigating the implication for mitochondrial involvement in ADPKD, we performed a mass spectrometry screen following GST pull-down of the p30 fragment in transfected HEK293t cells. We compared these results to GST alone transfected cells. Of the numerous mass spectrometry hits we received in the screen, two mitochondrial proteins appeared that were of particular interest, the ATP synthase β-subunit and apoptosis inducing factor (AIF).

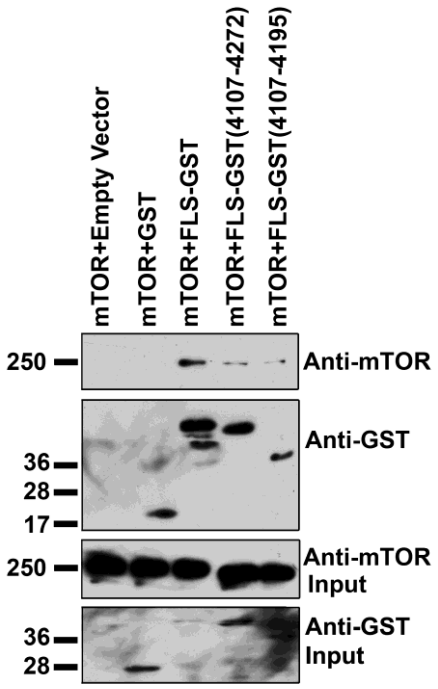

Figure 12: Interaction mapping between the C-terminus of PC1 and mTOR: HEK293t cells cotransfected with mTOR and GST tagged FLS/p30 (FLS-GST) truncation mutants of the C-terminus of FLS. mTOR binding was inhibited by deletion of the last 41 residues of FLS. Input=whole cell lysates

ATP Synthase β-Subunit

Following the mass spectrometry pull-down, I wanted to confirm the mass spectrometry interaction data via western blot. The ATP synthase β-subunit was intriguing because the interaction between the homolog of PC1, LOV-1 had been previously reported in *C. elegans*[109]. Hu et al reported that LOV-1 and the ATP synthase β-subunit were required for normal mating behavior with the interaction observed only in sensory neurons. This interaction was observed in a yeast to hybrid screen with the interaction in the PLAT domain of LOV-1, not the C-terminal tail and not in mitochondria. The PLAT domain is the most conserved region of PC1 and located 1000 amino acids away (AA 3107) from the C-terminus. The PLAT domain is associated with the membrane bound portion of

PC1 on the cytoplasmic side of the N-terminal GPI cleavage site. This may imply that the interaction with the ATPase may be used in regulating proton movement at the plasma membrane or an as yet unknown function of PC1.

HEK293t cells were transfected with p30 (FLS-GST) and probed for the ATP synthase β-subunit. Our lab has shown that the p30 fragment can be stabilized by inhibition of prolyl hydroxylase using either cobalt chloride or mimosine (unpublished). GST pull down revealed that binding to p30 was occurring to the ATP synthase β-subunit but was unaffected by treatment with cobalt chloride or mimosine (Fig. 13). I did not observe a stabilization of p30 as expected which may have been due to the fact this was an overexpression from transfection which may already be maximally expressing p30 and no further increase in protein is detectable. More experiments will need to be performed to verify this result and to test for a possible effect of this interaction.

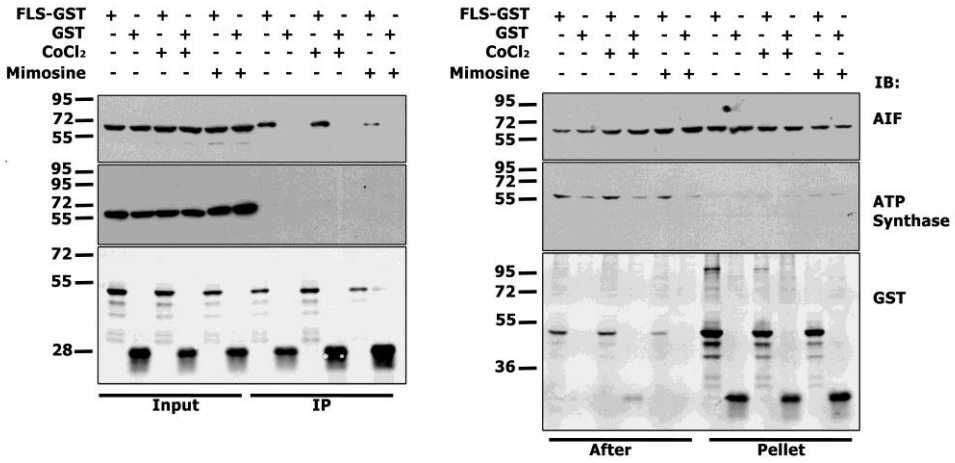

Figure 13: FLS Interacts with the ATP synthase β-subunit and Apoptosis Inducing Factor: HEK293t cells transfected with FLS-GST (p30) and subjected to GST pull-down following by immunoblotting of AIF and ATP synthase β-subunit wither with or without mimosine or cobalt chloride treatment. Input represents whole cell lysates, "After" represents depleted samples and "Pellet" represents all cellular fractions separated during centrifugation prior to GST pull down.

Apoptosis Inducing Factor

The other interesting mitochondrial protein obtained from the mass spec screen that showed a much stronger affinity for p30 (Fig.13) was AIF. AIF is localized to the inner mitochondrial membrane and is involved in caspase independent programmed cell death[110]. AIF is a Janus protein possessing FAD redox potential. AIF is tethered to the inner mitochondrial membrane by a proteolytically sensitive linker domain, sensitive to both calpain and cathepsin proteolysis. Cleavage of AIF can be caused by cellular insult from increases in calcium, ROS and DNA alkylating agents[111]. Following cleavage, AIF leaves the mitochondrion and translocates to the nucleus where it catalyzes chromatin condensation. While AIF does not possess endonuclease activity, its presence in the nucleus appears necessary for chromatin condensation[111]. AIF is translated as a 67kD pro-protein with an N-terminal mitochondrial localization sequence. Following translocation to the mitochondria, AIF is cleaved into the mature form with an apparent weight of 62kD. The N-terminal portion of the protein faces the mitochondrial matrix and the C-terminus faces the intermembrane space[112]. The N-terminal portion contains both FAD and NADH binding domains. AIF also exhibits oxydoreductase activity and is capable of reducing cytochrome C[111]. The function of AIF appears to be involved in regulation of complex 1 activity of the electron transport by regulation of ROS production[113]. Paradoxically, knockdown of AIF results in a 1.5-2 fold increase in ROS production in Hela cells and a decrease in in ROS activity in 5 other cell lines tested[113]. The difference may be explained by AIF modulation of complex 1 activity. AIF's role may be to regulate

the oxidation of complex 1 in response to ROS production, increasing activity by decreasing oxidation.

The association of a protein like AIF with the C-terminal tail of PC1 begs speculation about what the possible role of this interaction might be. In the immunoprecipitation assay (Fig. 13), the p30 fragment appears to associate strongly with AIF an enriched band that is of a slightly higher molecular weight than the band observed in the input samples. This may imply that the association of p30 and AIF is occurring in the cytoplasm or prior to the insertion of AIF into the mitochondrial inner membrane. This is an important distinction as the association of full length PC1 and the mitochondria has not been observed. However, our lab has observed that the p30 fragment appears to associate with structures that appear to be mitochondria under hypoxic conditions.

Recently the link between PC1 oxygen sensitivity and the mitochondria has been investigated. The association of PC1/PC2 in the ER and near the mitochondria is believed to be regulating calcium release from the ER for use in the mitochondria[114]. This is in conjunction with the prolyl hydroxylase EGLN3 that associates with the C-terminal tail of PC1 and regulates its trafficking to the plasma membrane under hypoxic conditions. Our lab has observed that prolyl hydroxylation is necessary for the regulation and degradation of the p30 fragment via the proteosome. It may be that the function of PC1 is to regulate the activity of the mitochondria via calcium regulation under normoxic conditions and then to prevent excessive ROS damage under hypoxic conditions. The association of PC1 and with the preprocessed form of AIF may serve as a regulation step for complex 1 activity.

Cell Death and Metabolism

After the confirmation between the association of p30 and AIF, I next checked if there was a cell death phenotype associated with p30 expression. To test this effect, an inducible MDCK cell line that expresses p30 following doxycycline administration. Using Alamar blue as a readout for cell death, I assayed for calcium induced cytotoxicity following ionomycin treatment. Comparing cell death at 24 hours under varying ionomycin concentration gave a dose of 500nM as an effective dose for killing cells (Fig. 14).

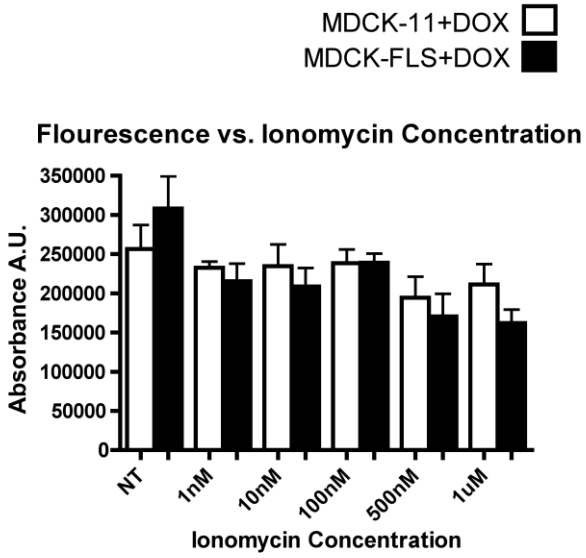

Figure 14: Alamar blue assay of ionomycin treated MDCK-FLS cells: MDCK cells stably expressing a doxycycline inducible version of p30 were exposed to varying concentrations of ionomycin 24 hours post ionomycin treatment to test for the effects on cell death.

The assay also revealed what appeared to be a possible increased effect on cell death from ionomycin in p30 expressing cells. To verify if there was an effect on cell death from p30 expression, I utilized another cell death assay that measures the amount of lactate dehydrogenase (LDH) released in the media from apoptotic

cells. LDH is normally an intracellular protein and should therefore not be in the media unless it is released from detached cells presumed to be apoptotic.

The LDH release assay revealed that there was a reduction in the amount of cell death observed in cells expressing p30 (Fig. 15), contradictory from the Alamar blue assay. The difference in outcomes is likely attributed to the difference in the way the assays measure cell death. The Alamar blue assay measures the reducing potential of the cells in culture to equate live cell activity. This measurement can be skewed if there is an effect in the cell that is altering cellular metabolism or redox reactions. If p30 is regulating a decrease in cellular metabolism in response to increased levels of calcium, it would be seen as a decrease in cell count via Alamar blue. The LDH release assay only measures the LDH that is released from cells that are apoptotic. Therefore, the LDH assay is a more reliable assay in terms of cell death and was used to measure the effects of ionomycin over time.

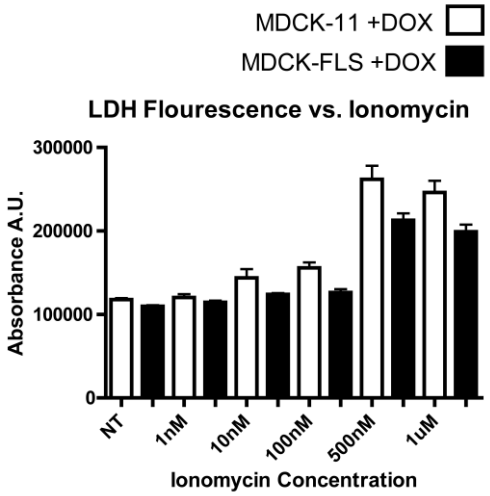

Figure 15: LDH release following ionomycin treatment in MDCK-FLS cells: MDCK cells stably expressing a doxycycline inducible version of p30 were exposed to varying concentrations of ionomycin 24 hours post ionomycin treatment.

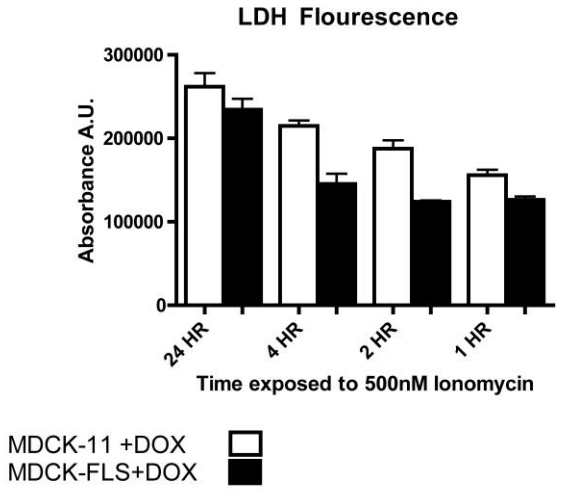

Figure 16: LDH release over time from ionomycin treated MDCK-FLS cells: MDCK cells stably expressing a doxycycline inducible version of p30 were exposed to 500nM ionomycin and assayed up to 24 hours post ionomycin treatment.

Taken together, these data imply that p30 may be involved in a yet unrecognized mechanism to regulate cellular metabolism and apoptosis following calcium toxicity. While it is not clear in what way this mechanism is taking place, it does look like p30 can protect against calcium induced cell death by regulating the cell's redox potential which may be to reduce toxic damage from reactive oxygen species. I next treated cells with 500nM ionomycin and measured the LDH release over time (Fig. 16). There was a marked effect in the amount of cell death measured after one hour and cells appeared to be resistant to cell death even after four hours of ionomycin treatment. These data suggest that p30 serves in a protective mechanism in calcium induced cytotoxicity possibly by regulating redox potential.

C. Discussion

The cytoplasmic tail of polycystin-1 appears to be quite promiscuous, involved in regulation of intracellular and mitochondrial calcium levels[114], gene coactivation[30], mTOR activity[29], and possible direct regulation of mitochondrial function. I have presented some interesting data and leads to follow. Of interest are the interactions between p30, mTOR and AIF. It would be worth to investigate if the interaction between mTOR and p30 is through a direct interaction or through a complex, if that interaction is preserved with the full-length PC1 protein, and if it serves any function.

The p30/AIF interactions beg speculation as AIF is directly involved in non-caspase mediated cell death and is activated by increased levels of intracellular calcium, and is involved in electron transport regulation. PC1 regulation by EGLN3 during hypoxia[114] make PC1 an oxygen sensor capable of regulating mitochondrial calcium levels by interacting with PC2 at the ER. This regulation of oxidative phosphorylation may also be as a direct regulator through complex 1 and/or 4 of the electron transport under hypoxic conditions by p30 interaction with AIF and the ATP synthase.

The C-terminal of PC1 binds with PC2 to form a calcium channel at the ER capable of regulating mitochondrial calcium levels and intracellular levels at the primary cilium by sensing fluid flow. Cleavage of the PC1 tail would presumably prevent the influx of calcium through PC1/2 disassociation. p30 cleavage is shown to occur in response to cessation of fluid flow from a lack of cilia bending. This could potentially result in a potentially hypoxic state as tubule obstruction can lead to decreased levels of oxygen. Association of p30 with the pro-form of AIF, prior

to its insertion into the mitochondrial membrane could prevent an increase in mitochondrial oxidative phosphorylation by disrupting membrane incorporation of AIF. This may make the C-terminal tail a signal for cellular oxygen status by integrating extracellular signals to the mitochondrial using AIF regulation.

The protective affect against ionomycin induced cytotoxicity may mean that p30 is regulating the effect of AIF induced cell death rather than its role in the electron transport chain. This effect may also be through electron transport regulation, preventing cellular damage. The location of the p30/AIF interaction needs to be determined first to make assumptions about possible functions.

IV.

The Ketogenic Diet as a Treatment for Autosomal Dominant Polycystic Kidney Disease

Abstract

The ketogenic diet has been shown effective in treating a number of metabolic and inflammatory diseases[115,116]. Ketosis causes the production of the ketone body β-hydroxybutyrate (βHB), a powerful signaling molecule, as a product of fatty acid metabolism. A ketogenic diet could counteract several important molecular targets in ADPKD as βHB has been shown to inhibit the activity of mTORC1[117], increase AMPK activation, is a known histone deacetylase (HDAC) inhibitor[118] and provides substrate for mitochondrial aerobic respiration[32]. ADPKD cysts show defects in aerobic fat metabolism with a concomitant shift to aerobic glycolysis[32], similar to a cancer cell's Warburg effect. mTORC1 is known to be upregulated in ADPKD and the mTOR inhibitor rapamycin has proven an effective treatment for ADPKD in rodent models[7,8]. Similarly, the use of HDAC inhibitors have shown promise in treating ADPKD[119] along with inhibition of aerobic glycolysis utilizing 2-deoxyglucose[32]. Taken together, the ketogenic diet may be a possible alternative to drug therapy for the treatment of ADPKD by decreasing overactive mTOR signaling and repairing the metabolic disease state in ADPKD.

A. Introduction

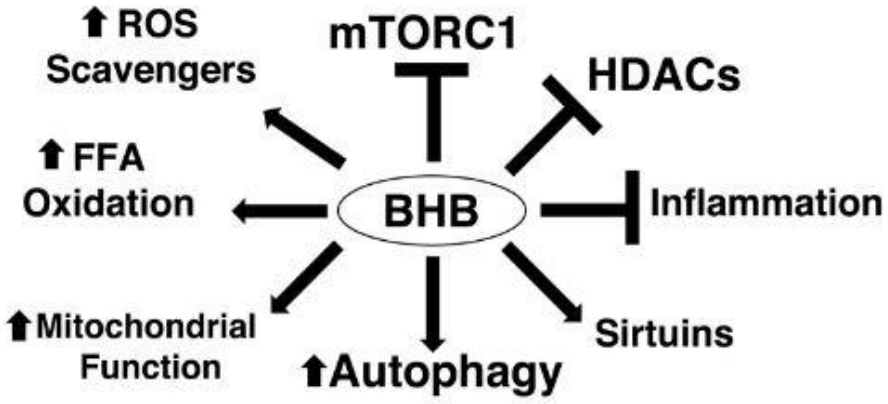

Figure 17: Pathways in ADPKD potentially affected by β-hydroxybutyrate: ADPKD pathways that are potentially affected by an increase in β-hydroxybutyrate.

Endogenous production of βHB occurs when employing a ketogenic diet and has already shown promise for the treatment of a number of metabolic and inflammatory diseases[115,120,121]. ADPKD exhibits several characteristics of metabolic and inflammatory diseases that make it an excellent candidate for treatment with a ketogenic diet. ADPKD patients are known to exhibit higher incidences of diabetes. Additionally, it has been shown that hyperglycemia is capable of exacerbating PKD following cilia ablation in the IFT88 knockout mouse[122]. The use of animal models to study ketosis has been well established utilizing supplementation with ketone esters[123], βHB salts[124], medium chain triglycerides[124], and macronutrient manipulation[121,124]. Ketosis has been utilized as a treatment for epilepsy[120], has been demonstrated to be safe and effective at treating inoperable tumors[116] and is currently being investigated for neurodegenerative diseases like Alzheimer's[125]. Taken together, the ketogenic diet

gives us an effective tool to begin studying the effects of ketosis on ADPKD progression.

Our lab recently published work demonstrating that caloric restriction is capable of ameliorating the cystic phenotype in mice with ADPKD[105]. The effects of caloric restriction on ADPKD may be due to several factors that come from the decrease in caloric intake. A decrease in caloric load leads to a state of ketosis, in which the body utilizes fat primarily for energy. The production of ketone bodies during times of caloric restriction not only provide energy, but also serve as potent signaling molecules for a number of pathways associated with ADPKD[5,9,14,15,16]. Ketogenesis produces three distinct ketone bodies: β-hydroxybutyrate, acetone and acetoacetate that each serves unique functions. Utilization of ketone bodies has been shown to boost expression of hypoxia inducing factor 1-alpha (HIF-1α) through an inhibition of prolyl hydroxylase activity, putatively via an increase in succinate[126]. βHB administration can act as a histone deacetylase class 1 and 2a inhibitor[127] while concomitantly activating Sirt1 acetylase activity[126] (Fig. 17). Ketosis also produces a more efficient use of oxygen and in animals is coupled to an increase in superoxide dismutase, catalase alongside a decrease in inflammasome markers of stress via AMPK activation[128]. Additionally, an increase in ketone bodies is shown to decrease mTORC1 activity while regulating an increase in macroautophagy and mitochondrial biogenesis[126,129]. Each of these pathways affected by ketosis has been targeted for therapeutic intervention in the treatment of ADPKD. Taken together, these data support the use of ketone bodies and the ketogenic diet as a potential alternative and effective treatment for ADPKD.

B. Results

To test the effect of the ketogenic diet on the progression of PKD, wild-type and PKD male and female Han:SPRD rats were treated for 5 weeks on a high-fat ketogenic diet beginning at 3 weeks of age. All the ketogenic diet treated animals were given ad libidum access to a high fat paste consisting of corn oil, lard, casein and dextrose with a caloric ratio of 75% fat to 8% protein and 13% carbohydrates. This diet is contrasted and compared to the normal chow fed animals consisting of 60% calories from carbohydrates, 25% from protein and 15% from fat. The caloric ratios given to the ketogenic animals mimic those of humans practicing a ketogenic diet but with a further reduced protein consumption.

Upon examination of the kidneys, there was a marked decrease in the appearance of cysts in the ketogenic diet treated animals relative to the control normal chow fed animals (Fig. 18). There also appeared to be a decrease in the size of cysts observed by H and E. There was also a decrease in the overall kidney size that was commensurate with the wild-type controls. At the end of the 5-week study there was a significant reduction in the 2-kidney to bodyweight ratio in both male and females on the ketogenic diet in comparison to their normal chow controls (Fig. 19). The reduction in 2-kidney to body weight was relative to the normal chow fed controls in the wild-type and PKD animals. This indicates that the reduction in the 2-kidney to bodyweight ratio in PKD animals is not due solely to an overall reduction in total organ growth per se. It should be noted that there was a dramatic reduction in the size of the animals following the 5-week period on the ketogenic diet relative to the normal chow fed controls (Fig. 20A).

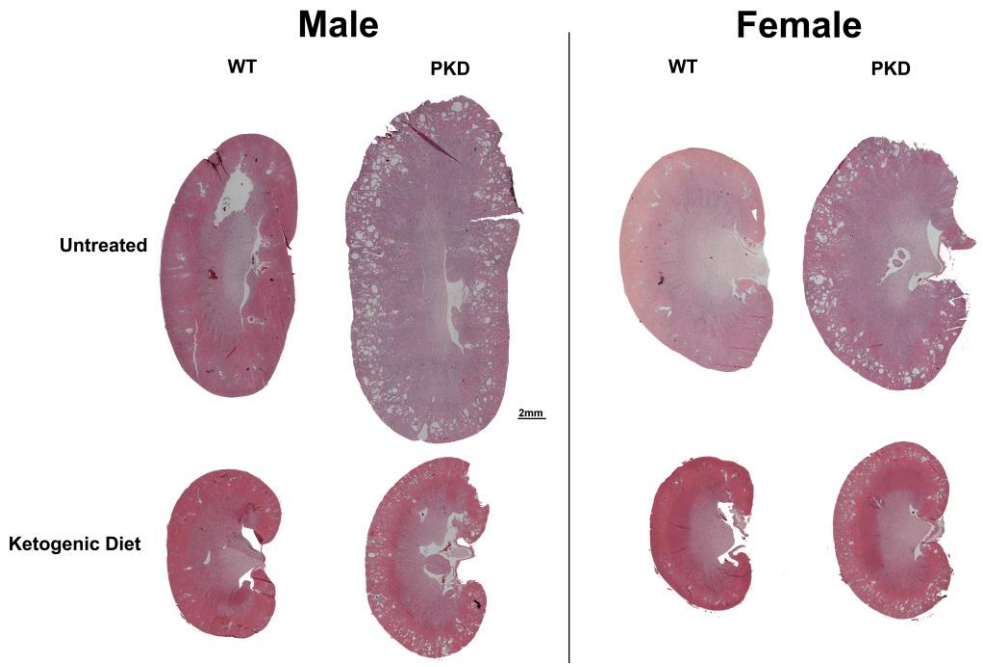

Figure 18: Hematoxylin and Eosin stain of ketogenic and normal chow Han rats: 8-week-old polycystic and wild-type Han:SPRD male and female rats fed on either normal chow or a ketogenic diet.

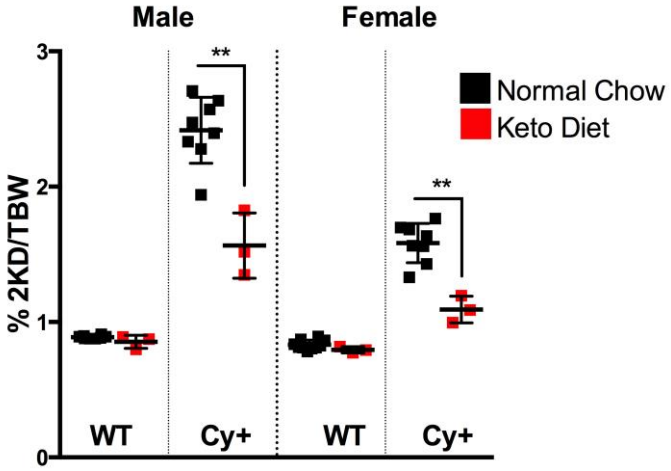

Figure 19: Two-kidney to bodyweight ratios of ketogenic and normal chow fed rats: 2-Kindey to bodyweight ratios of wild-type and polycystic Han rats treated with normal chow or a ketogenic diet.

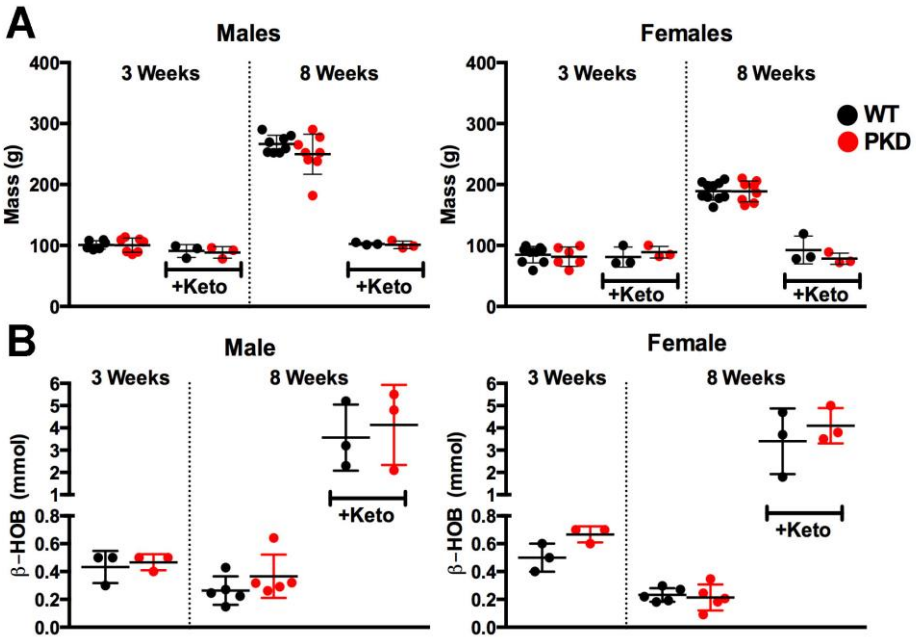

Figure 20: Mass and β-hydroxybutyrate measurements of ketogenic and normal chow Han rats over time: A.) Mass of wild-type and PKD male and female Han rats treated on the ketogenic diet or normal chow. **B.)** β-HOB levels of male and female wild-type and PKD Han rats.

Lack of tissue glycogen and the accompanied loss of associated water in addition to the decrease in protein are the most likely causes of the decreased mass of the animals treated with the ketogenic diet. As expected, there was an increase in βHB levels in the animals on a ketogenic diet relative to normal chow fed animals (Fig.20B).

When examining the individual animals over the course of the study, ketogenic treated animals increased by approximately 10%-15% in mass over the course of the study (Fig. 21A). This is contrasted to a more than doubling of the animals on normal chow diet in (Fig. 20A). This lack of growth is most likely due to the low protein content of the ketogenic formulation, making a consideration for a future study to optimize the protein content of the diet. Other than a decrease in the rats overall size, the ketogenic treated animals all appeared to be active and

in good health. All the animals on the ketogenic diet showed an increase in βHB levels over the 5-week period (Fig. 21B). Alongside the increase in βHB, there was a concomitant decrease in blood glucose levels observed in all animals (Fig. 21C).

To assess the function of the kidneys, blood urea nitrogen (BUN) levels were assayed in ketogenic and normal chow fed rats (Fig. 22). There was a marked reduction in all the ketogenic animal's BUN values compared to the normal chow fed controls. This decrease in BUN was observed in both the wild-type and the polycystic rats to a similar extent indicating that the effect of genotype was not as prominent as the effect of the ketogenic diet itself. Again, this decrease in BUN may be a cause of the low protein content rather than an effect of the diet per se. It is worth to note that this decrease in BUN may still offer palliative benefits by decreasing the filtration work output of the kidney.

To elucidate the signaling pathways that may affect cystic disease progression (Fig. 17), we analyzed signaling pathways identified in PKD (Fig. 23). There was a modest decrease in phospho-S6$^{S233/234}$ in ketogenic treated wild-type and PKD male rats. Unexpectedly, this is contrasted by an increase in phospho-S6$^{S233/234}$ observed in female PKD rats fed a ketogenic diet but does not appear to result in an increase in active phospho-4E-BP1. No change was observed in phospho-S6$^{S240/245}$. An increase in phospho-AMPK^{T172} was observed in all ketogenic treated animals relative to the normal fed chow PKD and wild-type rats.

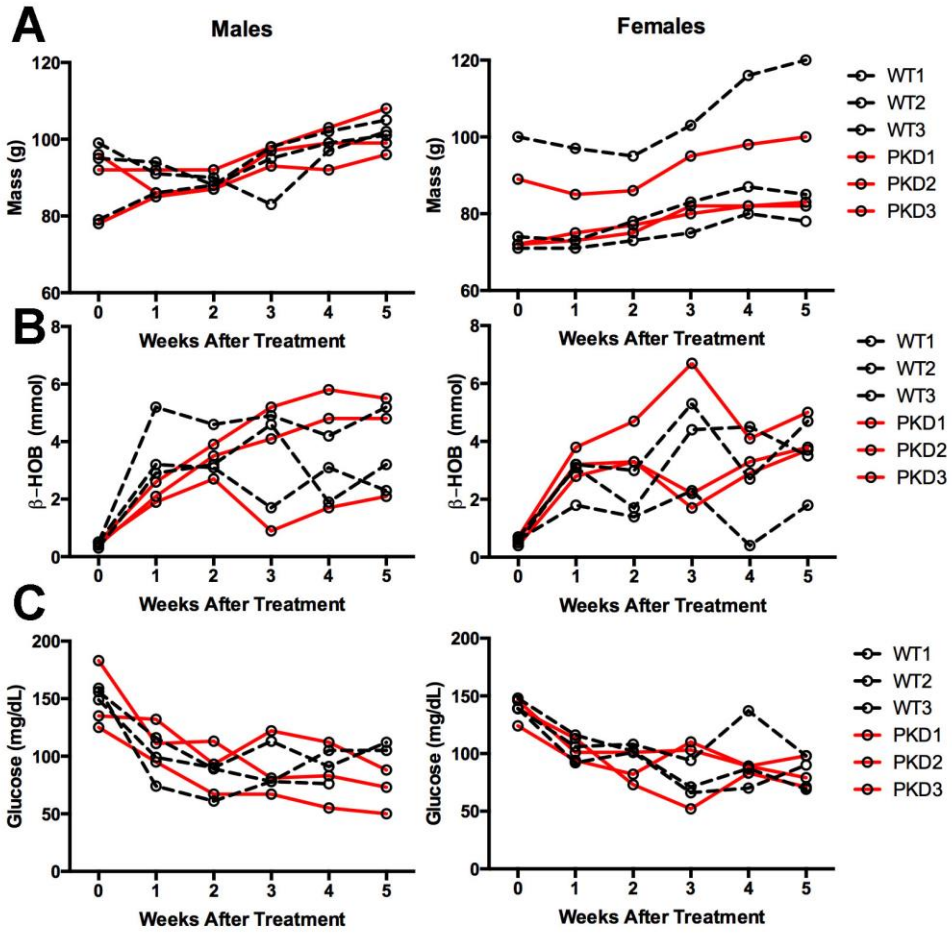

Figure 21: Weekly measurements of a single cohort of animals treated on the ketogenic diet: Rats were measured for A.) Mass, B.) β-hydroxybutyrate and C.) Blood glucose.

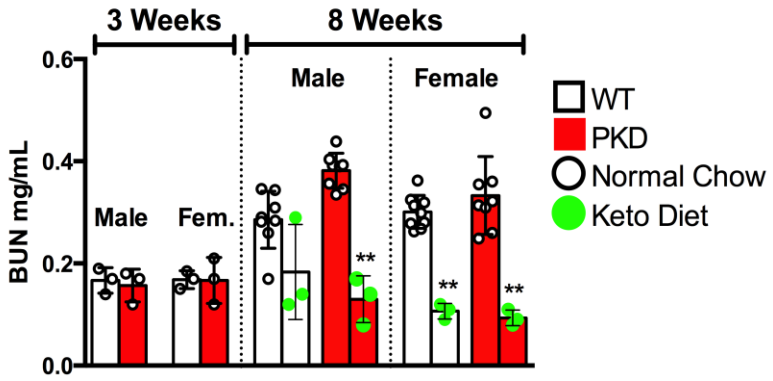

Figure 22: BUN levels of ketogenic and normal chow fed Han rats over time: BUN levels of PKD and wild-type rats on a ketogenic diet or normal chow. (**=P>0.01)

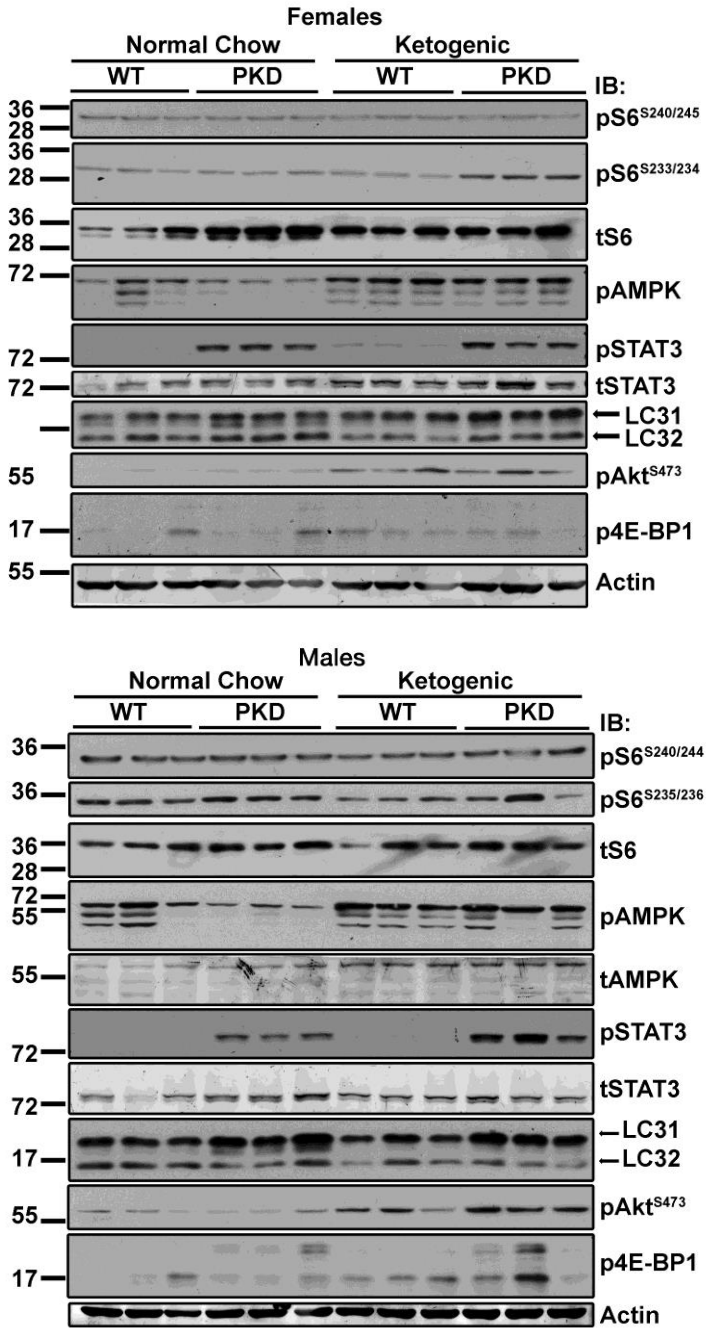

Figure 23: Western blot for ADPKD associated pathways in ketogenic and normal chow Han rat kidneys: 8-week old Han rat kidney lysates were probed for total and phosphorylated-S6$^{S233/234}$&$^{S240/245}$, total and phosphorylated-AMPK^{T172}, total and phosphorylated-STAT3^{Y705}, LC3, phosphorylated-Akt^{S473} and phosphorylated-4E-BP1. Actin was used as a loading control.

Another unexpected result was the increase in phospho-STAT3^{Y705} in the male and female ketogenic treated animals. Previously, our lab has used the appearance STAT3 as a marker of PKD and has been observed in models of PKD in the cyst lining epithelia. It is therefore difficult to speculate on the source or function of this increase. We examined the marker of autophagic flux, LC3, to assess if the lack of animal growth and the induction of ketosis coincided with an increase in autophagy. It appears that there is a difference between male and female rats in the active LC32 and pre-autophagic LC31 proteins. Male PKD rats appear to have more LC31 protein whereas females express more of the active LC32 form. In the ketogenic animals, there does appear to be an increase in the overall levels of LC1 levels relative to wild-types, with female PKD rats showing an increase in LC32. Phosphorylation of S473 of Akt is associated with mTORC2 activity[130] indicating that the ketogenic diet appears to increase mTORC2 activity in both males and females.

The changes in signaling for animals on the ketogenic diet showed some expected changes with an increase in mTORC2 and AMPK. Unexpectedly, there were differences in males and females on a ketogenic diet. This sex specific difference will require exploring further.

C. Discussion

The ketogenic diet has grown from being used for the treatment of epilepsy, to currently being researched for the treatment of neurodegenerative and metabolic disorders[125,131]. The renewed interest in ketosis has sparked =because of the powerful effects on cellular signaling and metabolism that can be elicited from the ketogenic state. The profound effects of the diet are linked primarily to the

production of the ketone body, β-hydroxybutyrate (βHB). βHB has been shown to play a central role in the effects observed while in ketosis, serving as a substrate for mitochondrial aerobic oxidation and as a transcriptional regulator[117]. Amongst the regulatory effects of βHB is its ability to inhibit mTORC1 via AMPK activation. AMPK is downregulated in PKD along with a concomitant increase in mTORC1 activity. mTOR inhibitors have shown therapeutic potential in rodent models of ADPKD but have not fared well in human trials. Since βHB is produced endogenously in the ketogenic state, this makes βHB an appealing alternative for ADPKD treatment over mTOR inhibitors.

In the current study, there was a nearly 20-fold increase in the levels of βHB for animals on a ketogenic diet at the end of the 5-week period (Fig. 20). This was accompanied by an expected increase in phosphorylated AMPK for all animals in ketosis. The increase in AMPK activation paradoxically was accompanied by an apparent increase in mTORC1 and mTORC2 signaling. AMPK is responsible for inhibition of mTORC1 through the phosphorylation of Raptor, the binding partner of mTOR necessary for complex 1 formation, phosphorylation of Raptor prevents complex 1 assembly. AMPK also targets the upstream regulator of mTORC1 activation, TSC2, which subsequently inhibits the GTPase Rheb, additionally disrupting the assembly of the mTORC1 complex[132]. Activation of 4E-BP1 by phosphorylation is a direct downstream target of mTORC1 and showed an increase in ketogenic diet male rats (Bottom Fig. 23). This was accompanied with an increase of Akt^{S473} phosphorylation, a marker for mTORC2 activity (Fig. 23). The increase in both mTORC1and mTORC2 activity appears to conflict as each complex act as a negative regulator of the other.

Explanation for the simultaneous activity of mTORC1/2 may be the upstream regulation of PTEN by the Hippo pathway. The Hippo pathway is involved in the regulation of organ size by controlling apoptosis and proliferation. Extracellular growth signals integrate and stabilize the transcription factor, Yes-Associated Protein (YAP). YAP is responsible for the transcription of miR-29, a negative regulator of PTEN translation. Decreased PTEN activity leads to an increase of PtdIns(3,4,5)P_3 via PI3K[133], which, in turn will lead to an activation of both the mTOR 1 and 2 complexes. This would match the observation of a decrease in autophagy, an increase in phosphorylated 4E-BP1, and the increase in Akt^{S473} phosphorylation.

The activity of Hippo would indicate that the signal for growth is in place without the needed substrate to proceed. The lack of growth in the animals may be entirely due to a lack of necessary nutrients to proliferate new cells. A lack of amino acids may impair the increase in animal size. Hippo has been shown to be dysregulated in *Pkd1* null cyst epithelial cells by mislocalization of YAP and altered levels of downstream effectors[134]. Future experiments might include additional protein sources to overcome this growth deficiency by providing more substrate for protein synthesis in the form of essential amino acids. An increase in the cystic phenotype under these circumstances may implicate the role of the Hippo pathway as a direct regulator of cystogenesis in the Han rat. Despite the lack of growth, there was an observable decrease in cysts in the kidneys of PKD animals on the ketogenic diet and is worth further investigation.

V.

Future Directions and Conclusions

In summary, I have presented several novel findings. First is the finding that crystals can exacerbate cystogenesis in a rat model of ADPKD and demonstrates that there is an endogenous trigger for cystogenesis (Chapter II). This is a critical discovery in the PKD field and shifts the emphasis away from researching drug targets and towards a possible therapeutic intervention that involves dietary modification. The field has come a long way in elucidating the function of the polycystins, cilia and the role they play in cyst formation. Second, I was able to demonstrate novel interactions of the cytoplasmic tail of PC1 with the mitochondrial proteins AIF and ATP synthase β-subunit along with the protein kinase mTOR. p30 is also involved in an anti-apoptotic mechanism in response to calcium-induced toxicity (Chapter III). Finally, I showed that a ketogenic diet can reduce cyst formation in a rodent model PKD and may be able to serve as a possible therapeutic for human ADPKD (Chapter IV).

Each of these stories open fascinating new lines of investigation, and at the intersection of these separate projects lie powerful insights into the mechanisms of cystic disease progression, initiation and maintenance.

Signaling Mechanisms in ADPKD; Reactive Oxygen Species

Having demonstrated that crystals are capable of triggering cystogenesis, the next areas of research will need to elucidate the signaling mechanism underlying the transformation to a cyst. Amongst the most likely potential candidates for the upstream regulators of cyst formation are reactive oxygen species (ROS). Previous research has demonstrated that crystals activate the NAPDH oxidase enzyme in Madin-Darby Canine Kidney (MDCK) epithelial cells[135]. This increase of ROS has several implications in downstream effectors. Of potential interest is the

transcription factor hypoxia inducing factor 1-alpha (HIF1α). HIF1α is regulated by ubiquitin mediated protein degradation wherein ubiquitin attachment occurs by modification of proline residues that are hydroxylated in the presence of oxygen. The use of prolyl hydroxylase for the degradation of cellular proteins is also necessary for polycystin-1 protein regulation[114].

It is interesting to note that ischemia reperfusion is capable of upregulating HIF1α[136] and promoting cystogenesis in a *Pkd*-hypomorphic model of ADPKD[3]. HIF1α is seen upregulated in the Han:SPRD rat[137] with the increase of mTOR signaling implicated at increasing the levels of HIF1α. Inhibition of HIF1α following ischemia reperfusion has been shown to prevent the accumulation of fibrotic tissue in the kidney[136]. However, inhibition of HIF1α was not sufficient to prevent cystic disease progression in the Han:SPRD model of PKD[137]. This could be due to the overactive mTOR activity already observed in the Han model. The activity of PI3K and mTOR is sufficient to increase levels of HIF1α even under normoxic conditions[138]. It is worth noting that the ketogenic diet upregulates HIF1α but simultaneously inhibits mTOR activation which may account for why there was still a positive effect in the Han rat.

Fibrosis induced following ischemia may be mitigated by regulating overactive mTOR signaling. The use of the rapalog sirolimus, has been shown to be effective in ameliorating cystic disease in the Han rat[139]. Sirolimus affects both the mTORC1 and mTORC2 complexes, which would influence other pathways including autophagy and regulation of cell size, making it difficult to say what the effect is from. Other studies have shown that rapamycin and inhibitors that effect S6K can also prevent interstitial fibrosis and cystic disease progression[140]. This

places mTOR signaling upstream of the development of cystic kidney disease and has been demonstrated by several labs with the use of rapalogs and various models of PKD[7,33,139].

The use of ROS scavengers in PKD has been shown to be insufficient in preventing PKD in the Lewis polycystic kidney (LPK) rat[141]. The LPK model is an ARPKD model with effects in the primary cilium. Therefore, it may not be the best example of regulation of ROS in ADPKD.

Additional support for the role of ROS in PKD is the use of angiotensinogen inhibitors as a treatment in animal models of PKD[142]. Angiotensin signaling produces ROS through intracellular NADPH oxidase[143], similar to oxalate crystals. It may be that the role of PC1 in the injury response and the progression of PKD is its ability for oxygen sensation. This is exemplified by the ability of microcrystals to exacerbate PKD in the Han rat. Microcrystals produce ROS through the NADPH oxidase system, leading to the activation of the inflammasome and IL-1β secretion. The inflammatory response produced in this circumstance should be acute as the crystals are cleared out of the tubule lumen and away from activating ROS in cells. mTOR may be responsible for regulating this response under normal conditions and its overactivation leads to a runaway production of inflammatory cytokines and proliferation following injury.

The inhibition of mTOR signaling may in fact be the inhibition of the production of inflammatory mediators in response to injury. The production of IL-1β is a known mediator of inflammation, activating the innate immune response and a host of genes related to cell survival.

This becomes an interesting topic as the interplay between STAT signaling, mTOR, ROS and cystic kidney disease converge. We know that ischemic injury to the kidney leads to the production of ROS; this in turn increases the levels of HIF1α and p30. ROS is also capable of activating the caspase-1 inflammasome leading to the production of IL-1β. IL-1β in turn activates even more ROS production in neighboring cells leading to increased inflammation. The production of IL-1β can be mediated by the mTORC1 complex, reducing the effect of inflammation. p30 increases along with the increase in ROS due to the hypoxic conditions of the cell. This in turn sensitizes cells to the effects of STAT3 signaling to initiate repair and proliferative responses. The C-terminal tail of PC1 contains a caspase-1 cleavage site which creates a small bioactive fragment that is still capable of coactivating STAT3 gene activity. The function of this cleavage may be to interfere with p30 interaction with other key regulatory molecules or to create new interactions that p30 can regulate under inflammatory conditions. In cystic kidney disease, the regulation of these critical pathways by PC1 is no longer functioning. How this is occurring precisely is still under debate.

p30 and Apoptosis

After observing that p30 influences the survival of cells following calcium induced toxicity (Chapter III), it would be interesting to investigate this protective phenotype further. The role of PC1/PC2 as a calcium ion channel that interacts with a calcium sensitive protein like AIF along with PC1/PC2 regulating mitochondrial calcium levels under normoxic conditions opens exciting areas of exploration. It would also be interesting to understand if the interaction of the ATP synthase β-subunit is also involved in this mechanism of regulation. It is

intriguing to speculate that PC1 is involved in the regulation of oxidative phosphorylation at the level of both complex one and ATP synthase by either sequestration of critical subunits or by effecting their trafficking to the mitochondria. The low abundance of ATPase associated with p30 may be because the right conditions have not been replicated to increase or stabilize binding. Replicating the experiment under hypoxic conditions utilizing the full length PC1 would be a great starting place. As of now, only the p30 fragment has been looked at for interacting with both AIF and the ATP synthase β-subunit. It would be interesting to test the ability of full length PC1 to bind to each of these proteins under both normoxia and hypoxia to see if they are differentially bound.

Future Directions

Future work on microcrystals would be to test the effect of stone preventative strategies for the treatment of PKD. Tanner et al showed that dietary citrate was able to improve the cystic phenotype in the Han rat[66]. Dietary intervention utilizing potassium citrate would act as a chelator of excess calcium, preventing the formation of any calcium dependent crystal. Reducing consumption of foods with large quantities of crystal forming agents (e.g. oxalate, phosphate, uric acid, calcium) could also be helpful in preventing disease progression. It would then make sense that PKD animals would exhibit increased markers of crystal precursors. Paradoxically, investigation into two mouse models of ADPKD showed no changes in lithogenic parameters[104]. This observation may be explained by the fact that mice are notoriously poor crystal formers, making them the wrong models to study this effect. There is, however, an increased incidence of crystal formation in ADPKD human patients and an increase in lithogenic

parameters[53,54]. It is therefore worth it to study the effects of crystal inhibition in a suitable model of PKD.

One of the problems with studying microcrystal induced PKD is the lack of an animal model orthologous to human ADPKD. The use of mice in genetic engineering has taken over the PKD field as the only models of PKD in rats have been discovered by random. It would therefore be prudent to produce an orthologous ADPKD rat model to study the effects of crystals on the progression of PKD. Creation of an inducible rat model of ADPKD would be a significant step in understanding the signaling of polycystin-1 following crystal deposition and allow for suitable tests to be done into the exploration of crystal induced PKD.

ROS appear to be center stage in PKD and in the interaction of crystals with the kidney. To test the effect of ROS and crystals on PKD, pretreatment with an ROS scavenger followed by increases in crystal forming agents should be able to prevent an increase in cystogenesis. Research into the effect of ROS in PKD has showed that depletion of glutathione can increase the amount of cystogenesis in the Han rat[144] and sodium thiosulfate has been shown to inhibit ethylene glycol induced hyperoxaluric renal damage by reducing oxidative stress in Wistar rats[145]. The link between kidney injury via ROS and the progression of PKD are unmistakable. It does appear that there may not be one singular cause of the generation of ROS that leads to PKD. Instead it appears that a combinatorial effect in the reduction of oxygen and the regulation of PC1 are explicably tied together in the pathogenesis of ADPKD. This decrease of oxygen can come from cellular signaling, increased aerobic metabolism or hypoxia. All of which cause the generation of ROS and a subsequent signaling cascade involving PC1.

Furthering the research into the effects of the ketogenic diet on PKD would be test the effect of the primary ketone body β-hydroxybutyrate (βHB). βHB can be supplemented as a powder that can be administered in the drinking water or in the feed. If the effects of the ketotic state are in fact a product of βHB signaling, then the supplementation of the βHB salt should be sufficient in protecting animals from disease progression.

To counteract the decreased weight gain seen in rats from a strict ketogenic diet may be to use a cyclical ketogenic approach. This type of ketogenic diet approach has been used because of increased sensitivity of insulin, growth hormone and mTOR signaling. This approach would allow for periodic "refeeds" in which animals eat more carbohydrates and protein before returning to a strict ketogenic diet. Modification of the dietary protein may also allow for the benefits of ketosis without the decreased weight gain.

Furthering the experiment, I presented here on the effect of ketosis in PKD would need to be repeated with an orthologous model of PKD, one that has a mutation in polycystin-1/2. This experiment is currently possible as mice are suitable to treat with a ketogenic diet.

Conclusion

During the tenure of my time as a graduate researcher, I investigated the mechanisms of PKD, beginning with studying the small soluble tail of PC1 followed by research into the possible endogenous injury mechanism for cyst formation. The search for the endogenous "third hit" in ADPKD led to the discovery of a yet unrecognized mTOR dependent mechanism that facilitates the removal of crystals in the kidney. The injury caused by microcrystals was shown

to be conserved amongst mice, rats and humans. With the discovery that microcrystals may exacerbate PKD, new therapeutic approaches can be investigated that target the initiation of cysts rather than trying to halt the progression of formed cysts.

The results obtained from the experiments with ethylene glycol treated rats showed that microcrystals can exacerbate the rate of cyst development. This was done in a sex specific manner, with males being affected over females. Crystal deposition appears necessary for cystogenesis as cystic females appeared unaffected and did not show crystal deposition. This finding shows that there is a possibility for therapeutic intervention utilizing dietary citrate as a calcium chelator and alkalinizing agent alongside other dietary recommendations to reduce and eliminate stone forming agents in the urinary filtrate. By increasing the intake of water, alkalinizing foods and compounds such as sodium bicarbonate along with removing foods with high levels of oxalate or protein may all be effective strategies to reduce the crystal burden in the kidneys. If the disease progression can be lengthened and the rate of cystogenesis can be modified so that the quality of life can be extended, it will effectively act as a cure for the disease until a time as a more specific therapy can be discovered. The biggest obstacle to the treatment of ADPKD is the systematic loss of healthy tissue due to the progression of cyst formation. Intervention that occurs early in life would able to preserve kidney function and circumvent the need for dialysis and transplant later in life.

Along with the finding that crystals exacerbate PKD, I demonstrated that a ketogenic diet may also be an effective intervention for the treatment of PKD. Both the dietary intervention to prevent stones and the ketogenic diet share

similarities in that they are aimed at reducing inflammation and the production of dangerous free radicals. If future research continues to remain positive, these treatments may one day be clinical approaches for the treatment of ADPKD.

VI. References

1. Knight, T. *et al.* Medical resource utilization and costs associated with autosomal dominant polycystic kidney disease in the USA: a retrospective matched cohort analysis of private insurer data. *Clin. Outcomes Res.* 123 (2015).

2. Weimbs, T. Third-hit signaling in renal cyst formation. *J. Am. Soc. Nephrol. JASN* **22,** 793–795 (2011).

3. Bastos, A. P. *et al.* Pkd1 haploinsufficiency increases renal damage and induces microcyst formation following ischemia/reperfusion. *J. Am. Soc. Nephrol. JASN* **20,** 2389–2402 (2009).

4. Happé, H. *et al.* Toxic tubular injury in kidneys from Pkd1-deletion mice accelerates cystogenesis accompanied by dysregulated planar cell polarity and canonical Wnt signaling pathways. *Hum. Mol. Genet.* **18,** 2532–2542 (2009).

5. Patel, V. *et al.* Acute kidney injury and aberrant planar cell polarity induce cyst formation in mice lacking renal cilia. *Hum. Mol. Genet.* **17,** 1578–1590 (2008).

6. Talbot, J. J. *et al.* Polycystin-1 regulates STAT activity by a dual mechanism. *Proc. Natl. Acad. Sci. U. S. A.* **108,** 7985–7990 (2011).

7. Shillingford, J. M., Piontek, K. B., Germino, G. G. & Weimbs, T. Rapamycin ameliorates PKD resulting from conditional inactivation of Pkd1. *J. Am. Soc. Nephrol. JASN* **21,** 489–497 (2010).

8. Shillingford, J. M. *et al.* The mTOR pathway is regulated by polycystin-1, and its inhibition reverses renal cystogenesis in polycystic kidney disease. *Proc. Natl. Acad. Sci. U. S. A.* **103,** 5466–5471 (2006).

9. Ong, A. C. M., Devuyst, O., Knebelmann, B. & Walz, G. Autosomal dominant polycystic kidney disease: the changing face of clinical management. *The Lancet* **385,** 1993–2002 (2015).

10. Torres, V. E., Harris, P. C. & Pirson, Y. Autosomal dominant polycystic kidney disease. *The Lancet* **369,** 1287–1301 (14).

11. Lentine, K. L., Xiao, H., Machnicki, G., Gheorghian, A. & Schnitzler, M. A. Renal Function and Healthcare Costs in Patients with Polycystic Kidney Disease. *Clin. J. Am. Soc. Nephrol. CJASN* **5,** 1471–1479 (2010).

12. Baur, B. P. & Meaney, C. J. Review of Tolvaptan for Autosomal Dominant Polycystic Kidney Disease. *Pharmacother. J. Hum. Pharmacol. Drug Ther.* **34,** 605–616 (2014).

13. Basten, S. G. & Giles, R. H. Functional aspects of primary cilia in signaling, cell cycle and tumorigenesis. *Cilia* **2,** 6 (2013).

14. Piontek, K., Menezes, L. F., Garcia-Gonzalez, M. A., Huso, D. L. & Germino, G. G. A critical developmental switch defines the kinetics of kidney cyst formation after loss of Pkd1. *Nat. Med.* **13,** 1490–1495 (2007).

15. Takakura, A. *et al.* Renal injury is a third hit promoting rapid development of adult polycystic kidney disease. *Hum. Mol. Genet.* **18,** 2523–2531 (2009).

16. Brown, J. H. *et al.* Missense mutation in sterile alpha motif of novel protein SamCystin is associated with polycystic kidney disease in (cy/+) rat. *J. Am. Soc. Nephrol. JASN* **16,** 3517–3526 (2005).

17. Yoder, B. K. *et al.* Polaris, a protein disrupted in orpk mutant mice, is required for assembly of renal cilium. *Am. J. Physiol. Renal Physiol.* **282,** F541-552 (2002).

18. Cai, Y. *et al.* Altered trafficking and stability of polycystins underlie polycystic kidney disease. *J. Clin. Invest.* **124,** 5129–5144 (2014).

19. Jones, C. *et al.* Ciliary proteins link basal body polarization to planar cell polarity regulation. *Nat. Genet.* **40,** 69–77 (2008).

20. Yoder, B. K., Hou, X. & Guay-Woodford, L. M. The Polycystic Kidney Disease Proteins, Polycystin-1, Polycystin-2, Polaris, and Cystin, Are Co-Localized in Renal Cilia. *J. Am. Soc. Nephrol.* **13,** 2508–2516 (2002).

21. Bell, P. D. *et al.* Loss of primary cilia upregulates renal hypertrophic signaling and promotes cystogenesis. *J. Am. Soc. Nephrol. JASN* **22,** 839–848 (2011).

22. Low, S. H. *et al.* Polycystin-1, STAT6, and P100 function in a pathway that transduces ciliary mechanosensation and is activated in polycystic kidney disease. *Dev. Cell* **10,** 57–69 (2006).

23. Takakura, A., Contrino, L., Beck, A. W. & Zhou, J. Pkd1 Inactivation Induced in Adulthood Produces Focal Cystic Disease. *J. Am. Soc. Nephrol. JASN* **19,** 2351–2363 (2008).

24. Watnick, T. *et al.* Mutations of PKD1 in ADPKD2 cysts suggest a pathogenic effect of trans-heterozygous mutations. *Nat. Genet.* **25,** 143–144 (2000).

25. Lantinga-van Leeuwen, I. S. *et al.* Kidney-specific inactivation of the Pkd1 gene induces rapid cyst formation in developing kidneys and a slow onset of disease in adult mice. *Hum. Mol. Genet.* **16,** 3188–3196 (2007).

26. Kurbegovic, A. & Trudel, M. Acute kidney injury induces hallmarks of polycystic kidney disease. *Am. J. Physiol. - Ren. Physiol.* **311,** F740–F751 (2016).

27. Weimbs, T. Polycystic kidney disease and renal injury repair: common pathways, fluid flow, and the function of polycystin-1. *Am. J. Physiol. - Ren. Physiol.* **293,** F1423–F1432 (2007).

28. Rogers, K. A. *et al.* Differences in the timing and magnitude of Pkd1 gene deletion determine the severity of polycystic kidney disease in an orthologous mouse model of ADPKD. *Physiol. Rep.* **4,** (2016).

29. Dere, R., Wilson, P. D., Sandford, R. N. & Walker, C. L. Carboxy Terminal Tail of Polycystin-1 Regulates Localization of TSC2 to Repress mTOR. *PLoS ONE* **5,** e9239 (2010).

30. Talbot, J. J. *et al.* The cleaved cytoplasmic tail of polycystin-1 regulates Src-dependent STAT3 activation. *J. Am. Soc. Nephrol. JASN* **25,** 1737–1748 (2014).

31. Lai, X. *et al.* Characterization of the renal cyst fluid proteome in autosomal dominant polycystic kidney disease (ADPKD) patients. *Proteomics Clin. Appl.* **2,** 1140–1152 (2008).

32. Riwanto, M. *et al.* Inhibition of Aerobic Glycolysis Attenuates Disease Progression in Polycystic Kidney Disease. *PLoS ONE* **11,** e0146654 (2016).

33. Zafar, I., Belibi, F. A., He, Z. & Edelstein, C. L. Long-term rapamycin therapy in the Han:SPRD rat model of polycystic kidney disease (PKD). *Nephrol. Dial. Transplant. Off. Publ. Eur. Dial. Transpl. Assoc. - Eur. Ren. Assoc.* **24,** 2349–2353 (2009).

34. Ruggenenti, P. *et al.* Effect of Sirolimus on Disease Progression in Patients with Autosomal Dominant Polycystic Kidney Disease and CKD Stages 3b-4. *Clin. J. Am. Soc. Nephrol. CJASN* **11,** 785–794 (2016).

35. Hanaoka, K. & Guggino, W. B. cAMP regulates cell proliferation and cyst formation in autosomal polycystic kidney disease cells. *J. Am. Soc. Nephrol. JASN* **11,** 1179–1187 (2000).

36. Wang, S. *et al.* Fibrocystin/polyductin, found in the same protein complex with polycystin-2, regulates calcium responses in kidney epithelia. *Mol. Cell. Biol.* **27,** 3241–3252 (2007).

37. Lager, D. J., Qian, Q., Bengal, R. J., Ishibashi, M. & Torres, V. E. The pck rat: a new model that resembles human autosomal dominant polycystic kidney and liver disease. *Kidney Int.* **59,** 126–136 (2001).

38. Masyuk, T. V. *et al.* Biliary dysgenesis in the PCK rat, an orthologous model of autosomal recessive polycystic kidney disease. *Am. J. Pathol.* **165,** 1719–1730 (2004).

39. Kaspareit-Rittinghausen, J., Rapp, K., Deerberg, F., Wcislo, A. & Messow, C. Hereditary Polycystic Kidney Disease Associated with Osteorenal Syndrome in Rats. *Vet. Pathol.* **26,** 195–201 (1989).

40. Cowley, B. D. *et al.* Autosomal-dominant polycystic kidney disease in the rat. *Kidney Int.* **43,** 522–534 (1993).

41. Erickson, K. F., Chertow, G. M. & Goldhaber-Fiebert, J. D. Cost-effectiveness of tolvaptan in autosomal dominant polycystic kidney disease. *Ann. Intern. Med.* **159,** 382–389 (2013).

42. Antignac, C. *et al.* The Future of Polycystic Kidney Disease Research—As Seen By the 12 Kaplan Awardees. *J. Am. Soc. Nephrol.* **26,** 2081–2095 (2015).

43. Schrier, R. W. *et al.* Predictors of autosomal dominant polycystic kidney disease progression. *J. Am. Soc. Nephrol. JASN* **25,** 2399–2418 (2014).

44. Milutinovic, J. *et al.* Intrafamilial phenotypic expression of autosomal dominant polycystic kidney disease. *Am. J. Kidney Dis. Off. J. Natl. Kidney Found.* **19,** 465–472 (1992).

45. Fain, P. R. *et al.* Modifier genes play a significant role in the phenotypic expression of PKD1. *Kidney Int.* **67,** 1256–1267 (2005).

46. Paterson, A. D. *et al.* Progressive loss of renal function is an age-dependent heritable trait in type 1 autosomal dominant polycystic kidney disease. *J. Am. Soc. Nephrol. JASN* **16,** 755–762 (2005).

47. Harris, P. C. & Rossetti, S. Determinants of renal disease variability in ADPKD. *Adv. Chronic Kidney Dis.* **17,** 131–139 (2010).

48. Grantham, J. J. *et al.* Detected renal cysts are tips of the iceberg in adults with ADPKD. *Clin. J. Am. Soc. Nephrol. CJASN* **7,** 1087–1093 (2012).

49. Robertson, W. G. A method for measuring calcium crystalluria. *Clin. Chim. Acta Int. J. Clin. Chem.* **26,** 105–110 (1969).

50. Khan, S. R. & Kok, D. J. Modulators of urinary stone formation. *Front. Biosci. J. Virtual Libr.* **9,** 1450–1482 (2004).

51. Fogazzi, G. B. Crystalluria: a neglected aspect of urinary sediment analysis. *Nephrol. Dial. Transplant. Off. Publ. Eur. Dial. Transpl. Assoc. - Eur. Ren. Assoc.* **11,** 379–387 (1996).

52. Khan, S. R. Calcium oxalate crystal interaction with renal tubular epithelium, mechanism of crystal adhesion and its impact on stone development. *Urol. Res.* **23,** 71–79 (1995).

53. Torres, V. E. *et al.* The association of nephrolithiasis and autosomal dominant polycystic kidney disease. *Am. J. Kidney Dis. Off. J. Natl. Kidney Found.* **11,** 318–325 (1988).

54. Dimitrakov, D. & Simeonov, S. Studies on nephrolithiasis in patients with autosomal dominant polycystic kidney disease. *Folia Med. (Plovdiv)* **36,** 27–30 (1994).

55. Torres, V. E., Wilson, D. M., Hattery, R. R. & Segura, J. W. Renal stone disease in autosomal dominant polycystic kidney disease. *Am. J. Kidney Dis. Off. J. Natl. Kidney Found.* **22,** 513–519 (1993).

56. Levine, E. & Grantham, J. J. Calcified renal stones and cyst calcifications in autosomal dominant polycystic kidney disease: clinical and CT study in 84 patients. *Am. J. Roentgenol.* **159,** 77–81 (1992).

57. Nishiura, J. L. *et al.* Evaluation of nephrolithiasis in autosomal dominant polycystic kidney disease patients. *Clin. J. Am. Soc. Nephrol. CJASN* **4,** 838–844 (2009).

58. Mejías, E., Navas, J., Lluberes, R. & Martínez-Maldonado, M. Hyperuricemia, gout, and autosomal dominant polycystic kidney disease. *Am. J. Med. Sci.* **297,** 145–148 (1989).

59. Panizo, N. *et al.* Chronic kidney disease progression in patients with autosomal dominant polycystic kidney disease. *Nefrol. Publ. Of. Soc. Esp. Nefrol.* **32,** 197–205 (2012).

60. Khan, S. R. & Glenton, P. A. Deposition of calcium phosphate and calcium oxalate crystals in the kidneys. *J. Urol.* **153,** 811–817 (1995).

61. Schäfer, K. *et al.* Characterization of the Han:SPRD rat model for hereditary polycystic kidney disease. *Kidney Int.* **46,** 134–152 (1994).

62. Nagao, S. *et al.* Increased water intake decreases progression of polycystic kidney disease in the PCK rat. *J. Am. Soc. Nephrol. JASN* **17,** 2220–2227 (2006).

63. Hopp, K. *et al.* Effects of hydration in rats and mice with polycystic kidney disease. *Am. J. Physiol. Renal Physiol.* **308,** F261-266 (2015).

64. Tanner, G. A. & Tanner, J. A. Dietary citrate treatment of polycystic kidney disease in rats. *Nephron Physiol.* **93,** P14-20 (2003).

65. Tanner, G. A. & Tanner, J. A. Citrate therapy for polycystic kidney disease in rats. *Kidney Int.* **58,** 1859–1869 (2000).

66. Tanner, G. A. Potassium citrate/citric acid intake improves renal function in rats with polycystic kidney disease. *J. Am. Soc. Nephrol.* **9,** 1242–1248 (1998).

67. Khan, S. R. & Glenton, P. A. Calcium oxalate crystal deposition in kidneys of hypercalciuric mice with disrupted type IIa sodium-phosphate cotransporter. *Am. J. Physiol. Renal Physiol.* **294,** F1109-1115 (2008).

68. Khan, S. R. & Glenton, P. A. Experimental induction of calcium oxalate nephrolithiasis in mice. *J. Urol.* **184,** 1189–1196 (2010).

69. Shillingford, J. M., Leamon, C. P., Vlahov, I. R. & Weimbs, T. Folate-conjugated rapamycin slows progression of polycystic kidney disease. *J. Am. Soc. Nephrol. JASN* **23,** 1674–1681 (2012).

70. Takakura, A. *et al.* Pyrimethamine inhibits adult polycystic kidney disease by modulating STAT signaling pathways. *Hum. Mol. Genet.* **20,** 4143–4154 (2011).

71. Leonhard, W. N. *et al.* Curcumin inhibits cystogenesis by simultaneous interference of multiple signaling pathways: in vivo evidence from a Pkd1-deletion model. *Am. J. Physiol. Renal Physiol.* **300,** F1193-1202 (2011).

72. Khan, S. R., Finlayson, B. & Hackett, R. L. Experimental calcium oxalate nephrolithiasis in the rat. Role of the renal papilla. *Am. J. Pathol.* **107,** 59–69 (1982).

73. Khan, S. R. & Hackett, R. L. Calcium oxalate urolithiasis in the rat: is it a model for human stone disease? A review of recent literature. *Scan. Electron Microsc.* 759–774 (1985).

74. Khan, S. R. & Hackett, R. L. Retention of calcium oxalate crystals in renal tubules. *Scanning Microsc.* **5,** 707-711-712 (1991).

75. Breljak, D. *et al.* In female rats, ethylene glycol treatment elevates protein expression of hepatic and renal oxalate transporter sat-1 (Slc26a1) without inducing hyperoxaluria. *Croat. Med. J.* **56,** 447–459 (2015).

76. Yoshioka, I. *et al.* Effect of Sex Hormones on Crystal Formation in a Stone-forming Rat Model. *Urology* **75,** 907–913 (2010).

77. Ward, C. J. *et al.* The gene mutated in autosomal recessive polycystic kidney disease encodes a large, receptor-like protein. *Nat. Genet.* **30,** 259–269 (2002).

78. Renken, C., Fischer, D.-C., Kundt, G., Gretz, N. & Haffner, D. Inhibition of mTOR with sirolimus does not attenuate progression of liver and kidney disease in PCK rats. *Nephrol. Dial. Transplant. Off. Publ. Eur. Dial. Transpl. Assoc. - Eur. Ren. Assoc.* **26,** 92–100 (2011).

79. Ren, X. S. *et al.* Activation of the PI3K/mTOR pathway is involved in cystic proliferation of cholangiocytes of the PCK rat. *PloS One* **9,** e87660 (2014).

80. Sweeney, W. E., von Vigier, R. O., Frost, P. & Avner, E. D. Src inhibition ameliorates polycystic kidney disease. *J. Am. Soc. Nephrol. JASN* **19,** 1331–1341 (2008).

81. Otnes, B. Sex differences in the crystalline composition of stones from the upper urinary tract. *Scand. J. Urol. Nephrol.* **14,** 51–56 (1980).

82. Khan, S. R. Renal tubular damage/dysfunction: key to the formation of kidney stones. *Urol. Res.* **34,** 86–91 (2006).

83. Vervaet, B. A., Verhulst, A., D'Haese, P. C. & De Broe, M. E. Nephrocalcinosis: new insights into mechanisms and consequences. *Nephrol. Dial. Transplant. Off. Publ. Eur. Dial. Transpl. Assoc. - Eur. Ren. Assoc.* **24,** 2030–2035 (2009).

84. Evan, A. P. *et al.* Mechanism of formation of human calcium oxalate renal stones on Randall's plaque. *Anat. Rec. Hoboken NJ 2007* **290,** 1315–1323 (2007).

85. Evan, A., Lingeman, J., Coe, F. L. & Worcester, E. Randall's plaque: pathogenesis and role in calcium oxalate nephrolithiasis. *Kidney Int.* **69,** 1313–1318 (2006).

86. Khan, S. R. Nephrocalcinosis in animal models with and without stones. *Urol. Res.* **38,** 429–438 (2010).

87. Khan, S. R., Finlayson, B. & Hackett, R. L. Histologic study of the early events in oxalate induced intranephronic calculosis. *Invest. Urol.* **17,** 199–202 (1979).

88. Worcester, E. M. *et al.* A test of the hypothesis that oxalate secretion produces proximal tubule crystallization in primary hyperoxaluria type I. *Am. J. Physiol. Renal Physiol.* **305,** F1574-1584 (2013).

89. Cornu, M., Albert, V. & Hall, M. N. mTOR in aging, metabolism, and cancer. *Curr. Opin. Genet. Dev.* **23,** 53–62 (2013).

90. Laplante, M. & Sabatini, D. M. mTOR signaling in growth control and disease. *Cell* **149,** 274–293 (2012).

91. Nishio, S. *et al.* Pkd1 regulates immortalized proliferation of renal tubular epithelial cells through p53 induction and JNK activation. *J. Clin. Invest.* **115,** 910–918 (2005).

92. Distefano, G. *et al.* Polycystin-1 regulates extracellular signal-regulated kinase-dependent phosphorylation of tuberin to control cell size through mTOR and its downstream effectors S6K and 4EBP1. *Mol. Cell. Biol.* **29,** 2359–2371 (2009).

93. Dalagiorgou, G. *et al.* Mechanosensor polycystin-1 potentiates differentiation of human osteoblastic cells by upregulating Runx2 expression via induction of JAK2/STAT3 signaling axis. *Cell. Mol. Life Sci. CMLS* (2016). doi:10.1007/s00018-016-2394-8

94. Mulay, S. R. *et al.* Cytotoxicity of crystals involves RIPK3-MLKL-mediated necroptosis. *Nat. Commun.* **7,** 10274 (2016).

95. Nagao, S. *et al.* Polycystic kidney disease in Han:SPRD Cy rats is associated with elevated expression and mislocalization of SamCystin. *Am. J. Physiol. - Ren. Physiol.* **299,** F1078–F1086 (2010).

96. Stagner, E. E., Bouvrette, D. J., Cheng, J. & Bryda, E. C. The polycystic kidney disease-related proteins Bicc1 and SamCystin interact. *Biochem. Biophys. Res. Commun.* **383,** 16–21 (2009).

97. Rothé, B. *et al.* Bicc1 Polymerization Regulates the Localization and Silencing of Bound mRNA. *Mol. Cell. Biol.* **35,** 3339–3353 (2015).

98. Lian, P. *et al.* Loss of polycystin-1 inhibits Bicc1 expression during mouse development. *PloS One* **9,** e88816 (2014).

99. Tran, U. *et al.* The RNA-binding protein bicaudal C regulates polycystin 2 in the kidney by antagonizing miR-17 activity. *Dev. Camb. Engl.* **137,** 1107–1116 (2010).

100. Wang, S., Wu, M., Yao, G., Zhang, J. & Zhou, J. The cytoplasmic tail of FPC antagonizes the full-length protein in the regulation of mTOR pathway. *PloS One* **9,** e95630 (2014).

101. Mattle, D. & Hess, B. Preventive treatment of nephrolithiasis with alkali citrate--a critical review. *Urol. Res.* **33,** 73–79 (2005).

102. Tanner, J. A. & Tanner, G. A. Dietary potassium citrate does not harm the pcy mouse. *Exp. Biol. Med. Maywood NJ* **230,** 57–60 (2005).

103. Tanner, G. A., Vijayalakshmi, K. & Tanner, J. A. Effects of potassium citrate/citric acid intake in a mouse model of polycystic kidney disease. *Nephron* **84,** 270–273 (2000).

104. Ferraz, R. R. N., Fonseca, J. M., Germino, G. G., Onuchic, L. F. & Heilberg, I. P. Determination of urinary lithogenic parameters in murine models orthologous to autosomal dominant polycystic kidney disease. *Urolithiasis* 1–7 (2014).

105. Kipp, K. R., Rezaei, M., Lin, L., Dewey, E. C. & Weimbs, T. A mild reduction of food intake slows disease progression in an orthologous mouse model of polycystic kidney disease. *Am. J. Physiol. - Ren. Physiol.* **310,** F726–F731 (2016).

106. Chauvet, V. *et al.* Mechanical stimuli induce cleavage and nuclear translocation of the polycystin-1 C terminus. *J. Clin. Invest.* **114,** 1433–1443 (2004).

107. Merrick, D. *et al.* The γ-secretase cleavage product of polycystin-1 regulates TCF and CHOP-mediated transcriptional activation through a p300-dependent mechanism. *Dev. Cell* **22,** 197–210 (2012).

108. Doerr, N. *et al.* Regulation of Polycystin-1 Function by Calmodulin Binding. *PloS One* **11,** e0161525 (2016).

109. Hu, J. & Barr, M. M. ATP-2 Interacts with the PLAT Domain of LOV-1 and Is Involved in Caenorhabditis elegans Polycystin Signaling. *Mol. Biol. Cell* **16,** 458–469 (2005).

110. Candé, C. *et al.* Apoptosis-inducing factor (AIF): a novel caspase-independent death effector released from mitochondria. *Biochimie* **84,** 215–222 (2002).

111. Delavallée, L., Cabon, L., Galán-Malo, P., Lorenzo, H. K. & Susin, S. A. AIF-mediated caspase-independent necroptosis: A new chance for targeted therapeutics. *IUBMB Life* **63,** 221–232 (2011).

112. Otera, H., Ohsakaya, S., Nagaura, Z.-I., Ishihara, N. & Mihara, K. Export of mitochondrial AIF in response to proapoptotic stimuli depends on processing at the intermembrane space. *EMBO J.* **24,** 1375–1386 (2005).

113. Polster, B. M. AIF, reactive oxygen species, and neurodegeneration: a 'complex' problem. *Neurochem. Int.* **62,** 695–702 (2013).

114. Padovano, V. *et al.* The polycystins are modulated by cellular oxygen-sensing pathways and regulate mitochondrial function. *Mol. Biol. Cell* **28,** 261–269 (2017).

115. Choi, I. Y. *et al.* A Diet Mimicking Fasting Promotes Regeneration and Reduces Autoimmunity and Multiple Sclerosis Symptoms. *Cell Rep.* **15,** 2136–2146 (2016).

116. Woolf, E. C., Syed, N. & Scheck, A. C. Tumor Metabolism, the Ketogenic Diet and β-Hydroxybutyrate: Novel Approaches to Adjuvant Brain Tumor Therapy. *Front. Mol. Neurosci.* **9,** (2016).

117. Grabacka, M., Pierzchalska, M., Dean, M. & Reiss, K. Regulation of Ketone Body Metabolism and the Role of PPARα. *Int. J. Mol. Sci.* **17,** (2016).

118. Shimazu, T. *et al.* Suppression of Oxidative Stress by β-Hydroxybutyrate, an Endogenous Histone Deacetylase Inhibitor. *Science* **339,** 211–214 (2013).

119. Cebotaru, L. *et al.* Inhibition of histone deacetylase 6 activity reduces cyst growth in polycystic kidney disease. *Kidney Int.* **90,** 90–99 (2016).

120. NEBELING, L. C. & LERNER, E. Implementing A Ketogenic Diet Based on Medium-chain Triglyceride Oil in Pediatric Patients with Cancer. *J. Am. Diet. Assoc.* **95,** 693–697 (1995).

121. Ruskin, D. N., Kawamura, M. & Masino, S. A. Reduced pain and inflammation in juvenile and adult rats fed a ketogenic diet. *PloS One* **4,** e8349 (2009).

122. Sas, K. M. *et al.* Hyperglycemia in the absence of cilia accelerates cystogenesis and induces renal damage. *Am. J. Physiol. - Ren. Physiol.* **309,** F79–F87 (2015).

123. Ciarlone, S. L., Grieco, J. C., D'Agostino, D. P. & Weeber, E. J. Ketone ester supplementation attenuates seizure activity, and improves behavior and hippocampal synaptic plasticity in an Angelman syndrome mouse model. *Neurobiol. Dis.* **96,** 38–46 (2016).

124. Kesl, S. L. *et al.* Effects of exogenous ketone supplementation on blood ketone, glucose, triglyceride, and lipoprotein levels in Sprague-Dawley rats. *Nutr. Metab.* **13,** 9 (2016).

125. Henderson, S. T. Ketone bodies as a therapeutic for Alzheimer's disease. *Neurother. J. Am. Soc. Exp. Neurother.* **5,** 470–480 (2008).

126. McCarty, M. F., DiNicolantonio, J. J. & O'Keefe, J. H. Ketosis may promote brain macroautophagy by activating Sirt1 and hypoxia-inducible factor-1. *Med. Hypotheses* **85,** 631–639 (2015).

127. Tran, M. T. *et al.* PGC1α drives NAD biosynthesis linking oxidative metabolism to renal protection. *Nature* **531,** 528–532 (2016).

128. Bae, H. R. *et al.* β-Hydroxybutyrate suppresses inflammasome formation by ameliorating endoplasmic reticulum stress via AMPK activation. *Oncotarget* (2016). doi:10.18632/oncotarget.12119

129. Bough, K. J. *et al.* Mitochondrial biogenesis in the anticonvulsant mechanism of the ketogenic diet. *Ann. Neurol.* **60,** 223–235 (2006).

130. Sarbassov, D. D., Guertin, D. A., Ali, S. M. & Sabatini, D. M. Phosphorylation and Regulation of Akt/PKB by the Rictor-mTOR Complex. *Science* **307,** 1098–1101 (2005).

131. Goday, A. *et al.* Short-term safety, tolerability and efficacy of a very low-calorie-ketogenic diet interventional weight loss program versus hypocaloric diet in patients with type 2 diabetes mellitus. *Nutr. Diabetes* **6,** e230 (2016).

132. Shackelford, D. B. Unravelling the connection between metabolism and tumorigenesis through studies of the liver kinase B1 tumour suppressor. *J. Carcinog.* **12,** 16 (2013).

133. Shimobayashi, M. & Hall, M. N. Making new contacts: the mTOR network in metabolism and signalling crosstalk. *Nat. Rev. Mol. Cell Biol.* **15,** 155–162 (2014).

134. Happé, H. *et al.* Altered Hippo signalling in polycystic kidney disease. *J. Pathol.* **224,** 133–142 (2011).

135. Khan, A., Byer, K. & Khan, S. R. Exposure of Madin-Darby Canine Kidney (MDCK) Cells to Oxalate and Calcium Oxalate Crystals Activates Nicotinamide Adenine Dinucleotide Phosphate (NADPH)-Oxidase. *Urology* **83,** 510.e1-510.e7 (2014).

136. Hill, P. *et al.* Inhibition of hypoxia inducible factor hydroxylases protects against renal ischemia-reperfusion injury. *J. Am. Soc. Nephrol. JASN* **19,** 39–46 (2008).

137. Belibi, F. *et al.* Hypoxia-inducible factor-1α (HIF-1α) and autophagy in polycystic kidney disease (PKD). *Am. J. Physiol. Renal Physiol.* **300,** F1235-1243 (2011).

138. Déry, M.-A. C., Michaud, M. D. & Richard, D. E. Hypoxia-inducible factor 1: regulation by hypoxic and non-hypoxic activators. *Int. J. Biochem. Cell Biol.* **37,** 535–540 (2005).

139. Ravichandran, K., Zafar, I., Ozkok, A. & Edelstein, C. L. An mTOR kinase inhibitor slows disease progression in a rat model of polycystic kidney disease. *Nephrol. Dial. Transplant. Off. Publ. Eur. Dial. Transpl. Assoc. - Eur. Ren. Assoc.* **30,** 45–53 (2015).

140. Liu, C. *et al.* Concomitant use of rapamycin and rosiglitazone delays the progression of polycystic kidney disease in Han:SPRD rats: A study of the mechanism of action. *Am. J. Physiol. Renal Physiol.*

141. Ding, A. *et al.* Chronic treatment with tempol does not significantly ameliorate renal tissue hypoxia or disease progression in a rodent model of polycystic kidney disease. *Clin. Exp. Pharmacol. Physiol.* **39,** 917–929 (2012).

142. Ravichandran, K., Ozkok, A., Wang, Q., Mullick, A. E. & Edelstein, C. L. Antisense-mediated angiotensinogen inhibition slows polycystic kidney disease in mice with a targeted mutation in Pkd2. *Am. J. Physiol. - Ren. Physiol.* **308,** F349–F357 (2015).

143. Sachse, A. & Wolf, G. Angiotensin II-induced reactive oxygen species and the kidney. *J. Am. Soc. Nephrol. JASN* **18,** 2439–2446 (2007).

144. Torres, V. E., Bengal, R. J., Litwiller, R. D. & Wilson, D. M. Aggravation of polycystic kidney disease in Han:SPRD rats by buthionine sulfoximine. *J. Am. Soc. Nephrol.* **8,** 1283–1291 (1997).

145. Bijarnia, R. K., Bachtler, M., Chandak, P. G., van Goor, H. & Pasch, A. Sodium Thiosulfate Ameliorates Oxidative Stress and Preserves Renal Function in Hyperoxaluric Rats. *PLoS ONE* **10,** (2015).

VII. Appendix

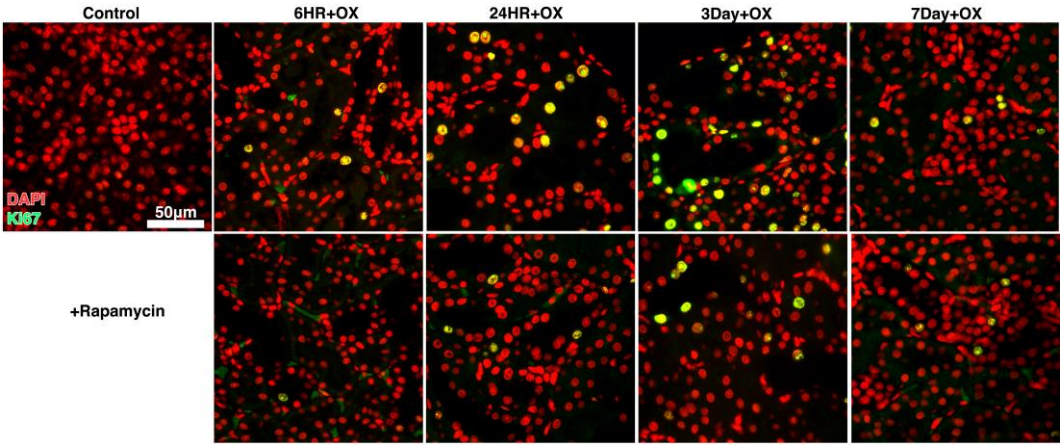

Supplemental Figure 1: **Ki-67 stained kidneys of rapamycin treated and control rats:** Wild-type Sprague Dawley rats were pretreated with rapamycin before IP injection of sodium oxalate. Animals were assessed for Ki-67 up to 7 days post treatment.

	Male		Female		p value	
	Control, 0.6%P (n=10)	HPD, 1.2%P (n=10)	Control, 0.6%P (n=10)	HPD, 1.2%P (n=10)	Diet	Gender
Body Weight (g)	387±20	345±12	245±13	228±8	<0.0001	<0.0001
Kidney Weight (g)	3.62±0.50	4.95±1.48	2.51±0.31	4.72±0.48	<0.0001	<0.0001
Kidney Weight (%BW)	0.94±0.14	1.44±0.44	1.02±0.10	2.08±0.22	<0.0001	0.0148
Kidney Cyst Score (%)	12.1±3.3	16.1±4.8	11.2±4.4	21.5±4.7	<0.0001	0.3784
Kidney Fibrosis Score (%)	3.2±1.6	6.6±2.0	3.8±1.5	12.3±2.1	<0.0001	0.1557
Renal Calcium deposits (%)	0.03±0.03	0.33±0.24	0.66±0.25	1.28±0.59	<0.0001	<0.0001
Serum Creatinine (mg/dl)	0.49±0.05	0.48±0.07	0.49±0.04	0.52±0.05	0.0127	0.0626
Serum BUN (mg/dl)	27.8±3.6	30.2±7.6	29.3±3.2	38.8±5.4	0.0026	0.1178
Serum Phosphorous (mg/dL)	8.9±1.1	7.5±2.6	9.9±0.4	7.7±1.0	0.0001	0.3699
Serum Calcium (mg/dL)	10.2±0.6	10.3±0.4	10.0±0.3	10.1±0.3	<0.0001	0.3163
Urine Creatinine (mg/dl)	94±55	128±39	88±34	132±32	<0.0001	0.7343
Urine Creatinine (mg/24hrs)	8.6±0.7	9.1±1.6	5.9±1.1	5.7±1.5	0.0011	<0.0001
Urine Phosphorous (mg/dl)	161±50	328±73	168±68	320±68	<0.0001	0.9852
Urine Phosphorous (mg/24hrs)	17.6±2.2	25.1±9.1	11.3±2.5	14.3±4.9	<0.0001	<0.0001
Urine Phosphorous (mg/g Creat)	2045±202	2720±683	1907±190	2486±463	<0.0001	0.185
Urine Phosphorous (mg/24hrs/100g BV	4.6±0.6	7.3±2.6	4.6±0.9	6.3±2.2	0.0004	0.4406
Urine Calcium (mg/dl)	36.4±24.2	67.5±31.5	44.4±17.9	51.0±19.9	<0.0001	0.7571
Urine Calcium (mg/24hrs)	3.3±0.7	4.6±1.3	3.0±0.4	2.3±0.9	<0.0001	0.623
Urine Calcium (mg/g Creat)	383±78	520±155	512±95	388±99	<0.0001	0.8066
Urine Calcium (mg/24hrs/100g BW)	0.85±0.18	1.35±0.39	1.22±0.20	1.00±0.43	<0.0001	0.6291
24 hrs Urine (ml)	11.2±4.4	8.4±5.0	8.0±3.9	4.8±2.3	0.0068	0.0537
Systolic BP(mmHg)	116±5	140±4	118±5	132±5	<0.0001	0.2316
Liver Weight (g)	16.2±1.3	14.5±1.5	10.3±0.5	9.8±0.3	<0.0001	<0.0001
Liver Weight (%BW)	4.18±0.22	4.21±0.34	4.19±0.14	4.29±0.23	<0.0001	0.2177
Liver Cyst Score(%)	5.6±3.0	6.2±1.7	5.7±2.5	7.1±1.3	0.2568	0.3742
Liver Fibrosis score (%)	3.9±0.8	3.1±1.0	4.9±0.8	5.0±1.1	0.0145	0.0001

Supplemental Table 1: **Animal measurements for high phosphate diet pck rats**: Male and female pck rats treated on either a high phosphate (1.2%) or normal phosphate (0.6%) diet were evaluated for markers of kidney performance.